FCTUC DEPARTAMENTO DE ENGENHARIA CIVIL
FACULDADE DE CIÊNCIAS E TECNOLOGIA
UNIVERSIDADE DE COIMBRA

Experimental and Numerical Investigation of the Static and Cyclic Fatigue of Laminated Glass

Dissertação apresentada para a obtenção do grau de Mestre em Engenharia Civil na Especialidade de Mecânica Estrutural

Autor
Ihor Yablonskyy

Orientador
Sandra Filomena da Silva Jordão
Jens Schneider

Coimbra, Janeiro, 2015

RESUMO

O vidro laminado é constituído por duas ou mais folhas de vidro coladas entre si por uma camada intermédia de plástico. Este sistema é usado cada vez mais em projetos de vidro estrutural devido às suas excelentes propriedades para transferir cargas e o seu conveniente comportamento pós quebra.

Além das comuns cargas estáticas de projeto, o vidro estrutural das fachadas também precisa ser capaz de suportar cargas ambientais e de impacto, que flutuam ao longo do tempo.

Com o os avanços científicos e tecnológicos, o vidro estrutural torna-se mais fino e mais económico, o que amplia os campos de uso, mas abre novas questões como o comportamento a longo prazo sob fadiga estática e cíclica de tais compostos estruturais. Fadiga cíclica é particularmente relevante para vidro estrutural, uma vez que ainda não tem sido tão amplamente estudada.

O objetivo desta dissertação é o de investigar o comportamento de vidro estrutural submetido á fadiga estática e cíclica. Isto será alcançado por meio de testes experimentais e modelos numéricos.

O cronograma de trabalho inclui, em primeiro lugar o estudo de fadiga dinâmica sobre vidro *float* e o comportamento do polyvinyl butyral (PVB) para pequenas extensões, de forma a definir as condições para os testes de grande extensão (fadiga) e, de seguida realizar os próprios testes de grande extensão. Finalmente, os modelos FEM são calibrados.

ABSTRACT

Laminated glass consists of two or more sheets of glass glued together by a plastic interlayer. This system is increasingly used in structural glass design because of its excellent properties to transfer loads and its convenient post breakage behavior.

Further to ordinary static design loads, structural laminates in facades also need to be able to withstand environmental and impact loads, which fluctuate through time.

With the advance of science and technology laminates become thinner and more economic, which broadens the fields of use, but opens new questions like the long term behavior under static and cyclic fatigue of such structural compounds. Cyclic fatigue is particularly relevant for laminates as it has not yet been as extensively studied.

The purpose of this master thesis is to investigate the laminates fatigue behavior for static and cyclic loading. This will be achieved by means of experimental tests and numerical models.

The work timeline encompasses firstly the study of dynamic fatigue on float glass and the small-strain behavior of the polyvinyl butyral (PVB), in order to define to define the conditions for the large-strain (fatigue) tests, and then to perform the actual large-strain tests. Finally the FEM models are calibrated.

ACKNOWLEDGEMENTS

To Prof. Dr. Sandra Filomena da Silva Jordão Alves, from University of Coimbra, for the eye-opening experience and the extensive help and support.

To Prof. Dr. Jens Schneider, from Technische Universität Darmstadt, for this great opportunity.

To Dipl. Ing. Jonas Hilcken, from Technische Universität Darmstadt, for the step by step support.

To my friends and colleagues for respectively moral support and technical advice.

To my family for their love and support.

INDEX

FIGURE INDEX

TABLE INDEX

1 INTRODUCTION

1.1 Preface

Today, engineers and architects are pushing the limits of glass by specifying the material in applications other than windows, such as floors, beams, walls, columns and roofs. Glass needs to be able to withstand environmental and impact loads, boosted several technological advancements like tempering laminating among others.

Although glass has already a respectable place in civil engineering it is still difficult to rely on it whole heartedly because of the uncertainty factor that it presents. Because of that a lot of time and money is invested in glass research in order to make it stronger, more secure or to find a way to make it more predictable.

The lamination technology is a clear example of that, since it has a huge interest in the industry. It consists of two or more sheets of glass glued together by a plastic interlayer. The system improves upon strength and ductility, furthermore the interlayer in case of failure holds the pieces together as to prevent them from falling on the pedestrians and cause damage.

The laminates become thinner and thus even more economic, which also broadens the fields of use, but opens new questions like the long term behavior under cyclic fatigue of such structural compounds. In fact structural glass components are subjected to periodically recurring loads throughout their lifetime, thus cyclic fatigue is a determinant aspect. Nevertheless, laminated glass is yet to be studied under cyclic fatigue. This thesis addresses this theme, following the cyclic fatigue study on float and heat tempered glass performed by Dipl. Eng. Jonas Hilcken at the Technical University of Darmstadt, Institute of Materials and Mechanics in Civil Engineering, Field of Expertise Static under the supervision of Professor Jens Schneider.

1.2 Framework

The cyclic fatigue is particularly relevant for laminated structural glass structures in the following situations:

- High-rise building's glass facades experiencing recurring wind loads

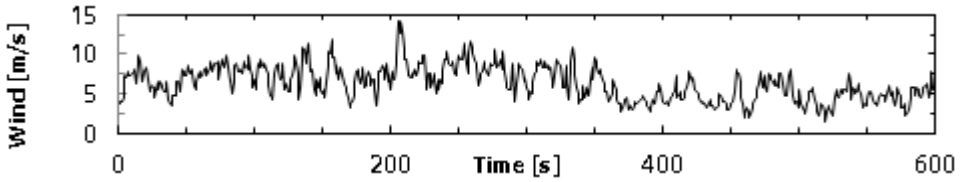

Figure 1.1 – Wind loads on high-rise buildings [20.]

- Acoustic panels of glass utilized on highways an railways, also experience recurring loads (pressure) provoked by the passing by vehicles

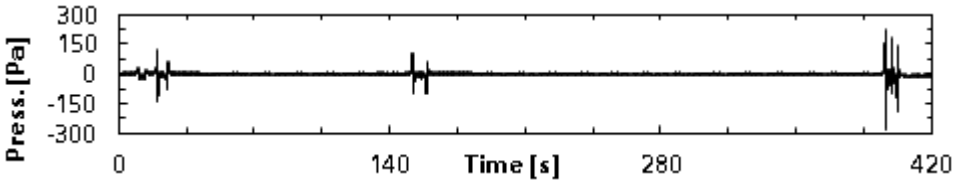

Figure 1.2 – Pressure provoked by the passing by vehicles [20.]

- Glass slabs and stairs experience recurring loads (deformation) provoked by mowing people

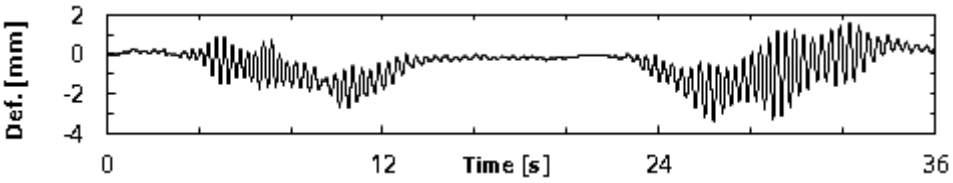

Figure 1.3 – Deformation provoked by mowing people [20.]

As referred above, cyclic fatigue is an aspect of structural glass design that has not yet been looked into. Only a few contributions have been put forward recently:

- Adhesive's behavior under cycling loading

Weller et al. [29.] performed a research on plastic adhesives for cyclic loading. The objective of the study was to identify the mechanical behavior of the adhesives. Therefore, three types of frequently used interlayers in structural glass applications were tested: Acrylate, Epoxy and Silicone.

First a preliminary test for a dynamic-mechanical analysis (DMA) was performed on all three adhesives in order to measure the temperature dependent viscoelastic behavior. By applying a oscillatory force the modulus of elasticity and the damping values are determined for a range of temperatures that (-20°C to 80°C)

The actual tests were performed for sinusoidal loading, during which the specimens were maintained in tension (Figure 1.4). The specimens were dog-bone shaped according to type 1B, with respective thickness of 4mm for Acrylate and Epoxy and 10mm for Silicone, fixed to a machine which provokes an axial force on the specimen (Figure 1.5). The strain variation was partially recorded via the dynamic extensometer or calculated from the relation between the accelerators position and the fixing length. The testing parameters were the frequency and the stress level (Table 1.1). For the frequency testing, in order for avoid rapid fatigue, the load was purposely set to be significantly lower than the adhesive's strength and for the stress level testing, the frequency was set at 5Hz while varying the load.

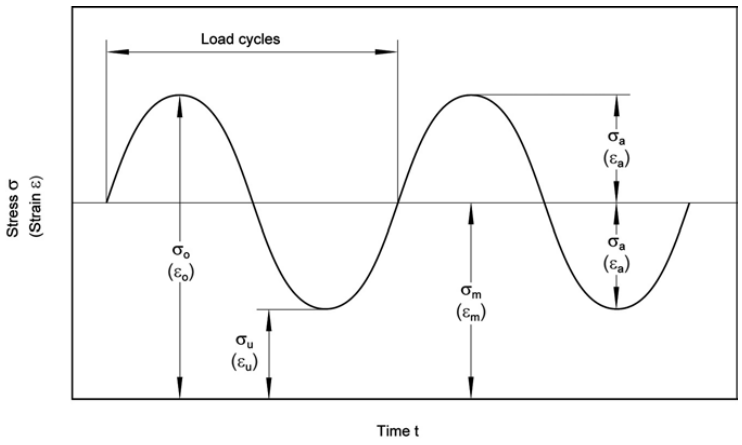

Figure 1.4 – Notations for fatigue testing according to DIN 50100 [29.]

Figure 1.5 – Test setup with the Acrylate specimen and dynamic extensometer [29.]

Table 1.1 Test parameters of the dynamic analysis [29.]

Adhesive	Frequency [Hz]	Minimum stress σ_u [N/mm²]	Maximum stress σ_o [N/mm²]
Acrylate	1 / 2 / 5 / 10 / 20 / 50	0.7	4.2
	5	0.7	2.1/ 4.2 / 6.3 / 8.4 / 10.5
Silicone	1 / 2 / 5 / 7.5	0.1	0.3
	5	0.1	0.3 / 0.4 / 0.5 / 0.6 / 0.7
Epoxy	1 / 2 / 5 / 10 / 20 / 50	1.5	9.1
	5	1.5	4.6 / 9.1 / 13.7 / 18.2 / 22.8

Although the three types of adhesives differ in their components and molecular structure, and the obtained results for strain and creep rates differ, they still exhibited similarities: in terms of creep deformations; growing stress increased the creep effects; failure and temperature development was the consequence of higher frequencies and stress levels; the adhesives material behavior was not influenced by low heating. Tested Acrylate, Silicone and highly stressed Epoxy, presented material softening.

- Glass's fatigue behavior under dynamic loading when in presence of induced flaws

Engel [13.] performed a research on the effects of induced flaws in terms of the statistical scatter of float glass's strength for different types of flaws. The objective was to find a type of induced flaw from which results the lowest possible statistical scattering and also allows a good reproducibility of the flaw.

The specimens (length: 240mm, width: 240mm, thickness: 4mm or 6mm) were damaged by means of: Glass Cutter, Corundum P16, Sandpaper P90, Indentation Test *UST* (60° Diamond), Penett-Cutter, Green Laser (532 nm wavelength) and CO2-Laser. The different types of flaws were analyzed and afterwards the specimens were tested in a dynamic way until failure for a constant strain-rate of 2MPa/s, for the Coaxial Double Ring (CDR) bending test (Figure 1.6).

Figure 1.6 – CDR bending test: load ring, r=43mm; support ring, r=72,5mm [13.]

In light of the results it was concluded that a good reproducibility of the flaw can be done by three means in the following order of importance: Penett-Cutter; 60° Diamond and the Glass Cutter. The results of this study may be utilized by the study of material fatigue of glass.

- Glass's fatigue prediction under cycling loading

Viehl [5.] performed a research on the fatigue behavior of float glass, with induced flaws, under cyclic load for the CDR bending tests (Figure 4.6). The objective of the study was to identify a suitable method, by means of a numerical model and an analytical formula, to predict the life time of the specimens (length: 250mm, width: 250mm). The specimens were induced with a flow via the Universal Surface Tester (UST 1000), where an indentation, via a 120° Diamond, was applied for a force and length of respectively 500mN and 2mm, after which the specimens experienced a resting period of 1 week. Two equations were analyzed: the empirically constructed *Power Law* and the *Paris Law* that is also used in ceramic predictions. The parameters of this study were as illustrated by Figure 1.7.

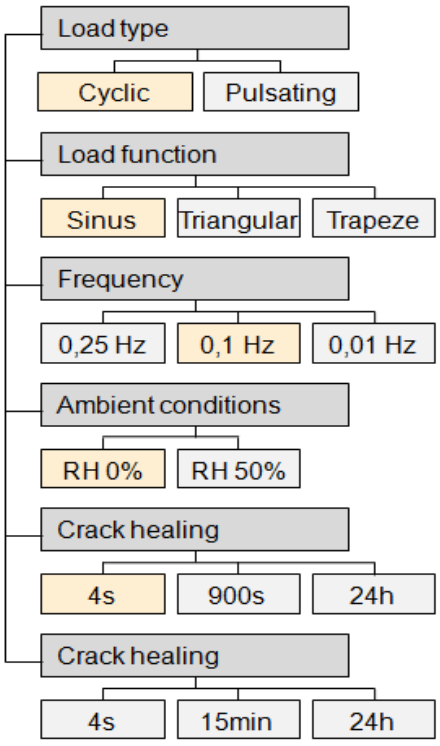

Figure 1.7 – Testing parameters

It was concluded that the *Power Law* was suitable to perform predictions for all of the studied parameters, whereas the *Paris Law* was only suitable for the crack healing and ambient parameters.

- Heat strengthened glass's fatigue behavior under cyclic loading

Hilcken [24.] performed a research on the fatigue behavior of heat strengthened glass exposed to cycling loading. For that matter CDR bending tests (Figure 4.6) for cycling fatigue were performed on the specimens (length: 250mm, width: 250mm). The specimens were induced with a flow via the Universal Surface Tester (UST 1000), where an indentation, via a 120° Diamond, was applied for a force and length of respectively 500mN and 2mm, after which the specimens experienced a resting period of 1 week. Also an analytical analysis via *Power Law* and a numerical model were performed for fatigue prediction. The fatigue behavior was studied for the parameters presented in Figure 1.8.

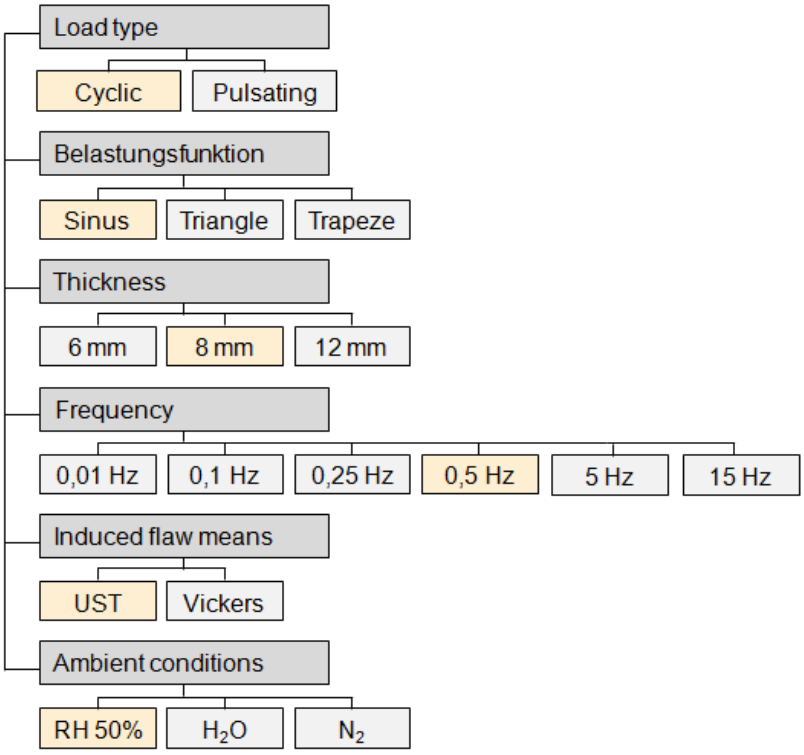

Figure 1.8 – Testing parameters [24.]

It was concluded that periodically recurring loads and the load history have a big impact on the durability and strength of the specimen. Crack propagation under cyclic loading is dominated by the time dependent processes and can be predicted with the current crack growth methods. The influence of the load and the ambient conditions on the cyclic fatigue can be derived from the static fatigue.

- Laminated glass's small-strain behavior under static loading

Sackmann et al. [19.] performed a research on the laminates behavior exposed to small-strain. The objective of this work was to investigate the PVB's material behavior, particularly its shear modulus, present in the laminate. Different types of conditions were studied, such as: load duration, temperature and ageing (through weathering by ultraviolet radiation and humidity).

The performed tests were:

- the four-point bending test (Figure 1.9) in order to study the influence of the load duration (short-term load with variable load, until 160s and long-term load with constant load, until 200h) and a temperature (constant temperature conditions in a climate chamber between 0°C and 60°C) on the structural behavior of laminates (spans: 1,0m and 2,0m; glass's thickness: 2x10mm and 2x4mm; PVB's thickness: 0,76mm; width: 0,36m).

- the four-point cyclic bending test in order to study a wind load simulation on laminates (span: 1,0m; glass's thickness 2x10mm and 2x4mm; PVB's thickness: 1,52mm) for the harmonic bending oscillation (of 10000 cycles) and a temperature (constant temperature conditions in a climate chamber: 0°C, 20°C, 40°C and 60°C)

- the shearing test (Figure 1.10) in order to study the influence for the ageing condition on the bond that the PVB provides to the laminate (length: 50mm; glass's thickness: 2x6mm, PVB's thickness: 1,52mm; width: 80mm) for an increase in shear force and a temperature (constant temperature conditions in a climate chamber between 5°C and 60°C).

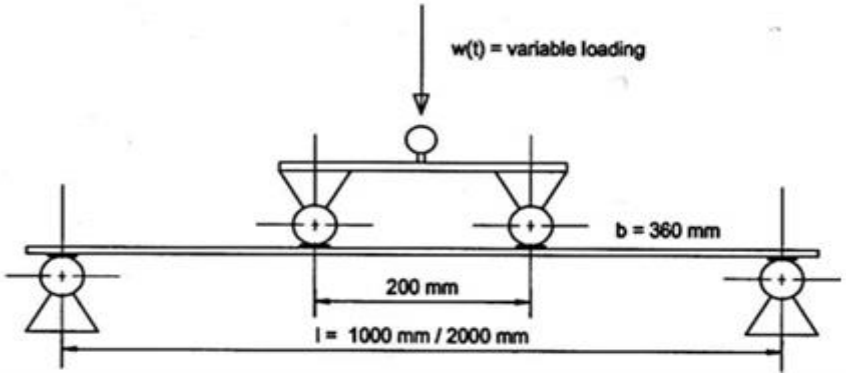

Figure 1.9 – Four-point bending test set-up [19.]

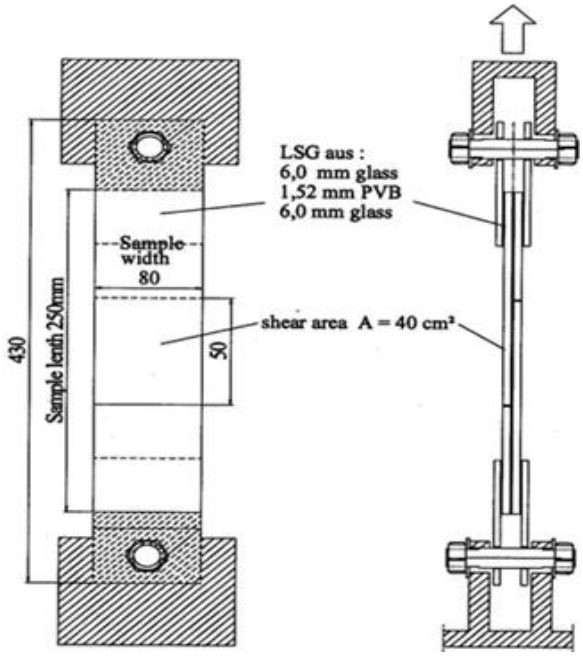

Figure 1.7 – Shearing test set-up for weathered specimens [19.]

It was concluded that PVB viscoelastic behavior affects the laminate when in presence of bending loads. Its shear bond is significantly influenced by the temperature and load duration. For small-strain the laminate presents a linear viscoelastic behavior. Long-term cycling loading shows no decrease in the bending stiffness. The shear bond of laminated glass is affected by the ageing.

The aim of the current thesis is within the framework of the PhD thesis of Dipl. Eng. Jonas Hilcken. Specifically it deals with the fatigue behavior of glass laminated with polyvinyl butyral (PVB) interlayer. In order to evaluate the mechanical behavior of the laminate experimental tests were performed and FEM models were developed. The experiments were performed by the coaxial double ring (CDR). The FEM models were verified by the experimental results. The tests were performed for small-strain and large-strain. “Dehnungsmessstreifen” (DMS) gauge stress chips were utilized for the small-strain test in order to evaluate the PVB interlayers mechanical behavior. On Float and laminated glass induced flaws were performed with a Universal Surface Tester (UST) with a diamond tip in order to respectively study the glasses and laminates fatigue behavior for large-strain.

1.3 Organization

This sub-chapter contains a brief summary of each chapter in this master thesis.

Chapter 2 provides some basic knowledge on the laminate and its constituents. The material and mechanical properties of float glass, PVB interlayer and laminated glass were discussed. The fundamental information on the experimental bending test and the fatigue prediction is transmitted.

Chapter 3 serves to verify the statements made throughout the Chapter 2, by means of the FEM tool *ANSYS Workbench.*
Chapter 4 deals with the preparations for the actual experiments, it also provides the experimental line up. It is in this chapter that the induced flaw and the crack velocity parameter were defined, which are going to be further implemented in Chapter 5 for fatigue prediction.

Chapter 5 encompasses the presentation and evaluation of results from the small-strain and large-strain experiments and the validation of the FEM models. Fatigue prediction for large-strain is also performed.

This thesis is completed with the Chapter 6, where the results are discussed. Furthermore follows an outlook on future research to which this thesis can serve as an incentive.

2 BASICS

2.1 Introduction

Since the dawn of time, mankind was always fascinated with the material known as glass. Depending of the necessities of the people, glass has always had its use, be it as a weapon (sharp cutting tool), an accessory or just a vessel. The process of making glass has continuously being perfected, as man strived to accommodate he's necessities. Even now a day's glass is being studied, researched and improved upon.

Glass exists naturally and is the product of super high temperatures originated from: volcanic activity (obsidian), lightning strikes (fulgurite) or the impact of meteorites (moldavite). The phenomena cause certain types of rocks or sand to melt, fuse, and then cool rapidly [26.]. It was first discovered by our forefathers and as it wasn't much transparent it was mainly used as a sharp cutting tool.

The first use of man-produced glass was as glazing and it was a decorative coating of glass enveloping a vessel made of another material. Some stone beads that used glass as a decorative coating have been found in Egypt and dated as early as 12,000 B.C [27.]. The manufacturing of glass begun around 1500 B.C. in Egypt and Mesopotamia and since then was forgotten, found and rediscovered by many civilisations, such as the Syrians, Romans, Byzantines, Venetians and others. The first colorless and transparent glass was manufactured by the Venetians.

The Industrial Revolution accompanied by the advancements in chemistry propitiated conditions for a lot of innovations in glass manufacturing. The process of glass making turned more automated and the glass's chemical composition was altered in order to turn it stronger and more heat-resistant. In 1871, William Pilkington invented a machine which automated the production of plate glass; this mechanized process was improved by J.H. Lubber in America in 1903 [28.].

It was at the beginning of the 20st century that heat tempering was discovered, it involves heating and then rapidly cooling at a constant rate. This rapid cooling result’s in a residual compressive stress on the glass's surface, which largely increases its strength.
In 1903 Eduard Benedictus, a French chemist, by a struck of luck observed a laboratory accident in which a glass flask coated in the plastic cellulose nitrate dropped and shattered, but did not break into pieces [14.].

Polyvinyl Butyral (PVB) has been the dominant interlayer since the late 1930s. In 1950s it was heavily used in the automobile safety glass and later also as a civil engineering material [15.].

In the 1950s the float process was developed by Alastair Pilkington, changing glass manufacturing forever. The cost of glass drove down and new applications were created, such as the facades of high-rise office buildings.

2.2 Float Glass

The most common process of producing glass is called “float process”, which accounts 90% of today’s flat glass production. As before mentioned, in 1959 float glass process was commercially introduced by the Pilkington Brothers. The main attractiveness of float glass is its low cost, its superior optical quality, its smooth surface for silicate glass and the large size of panes that can be reliably produced.

The process of manufacturing the float (annealed) glass [1.] consists of 3 stages (Figure 2.1): The 1st stage involves the melting of the raw materials in a furnace at temperatures of up to 1550°C; in the 2nd stage, the molten glass is poured continuously at approximately 1000°C on to a shallow pool of molten tin, where the glass floats without mixing with the tin because of its lower specific weight, and then spreads outwards forming a smooth flat surface where it gradually cools down and is drawn on to rollers (the 3rd stage); in the 3rd and last stage the glass enters the large oven, called *lehr*, at around 600°C where the glass is slowly cooled down until 100°C as means to prevent residual stresses being induced within the glass. The glass's thickness is regulated by the velocity of the rollers present in the 3rd stage, that is, the lower the velocity the higher the thickness of the glass and vice-versa. At the end the glass gets to be is inspected and then cut in typical size.

By using float glass in load bearing elements it is usually required to strengthen it, which gave birth to tempering and laminating.

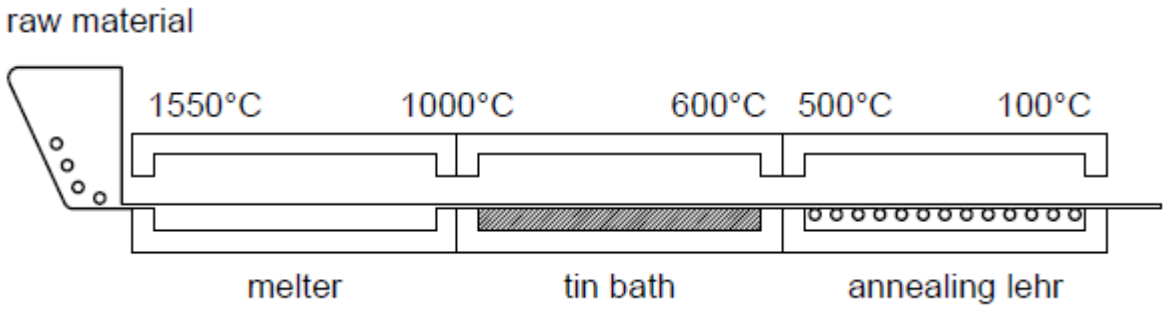

Figure 2.1 – Float glass process [1.]

2.2.1 Material Properties of Float Glass

Glass is an “inorganic product of fusion which has been cooled to a rigid condition without crystallization” [1.]. It is a homogenous, isotropic and linear-elastic material with no feasible plastic capacity. It's a perfectly brittle material and has the advantage of rigorously following Hook's law at ambient temperatures. The most common glass used in civil engineering is soda lime silica glass (SLSG) and as all non-crystalline solids it doesn’t present an ordered pattern in its constitution (Figure 2.2).

Glass is a particular solid, it doesn't absorb nor dissipate the radiation in bandwidths of visible and near infrared and that is why glass is so transparent. What make’s glass so special are the molecules electrons, which are strictly confined to particular energy level and as a consequence they cannot absorb those radiations and alternate between different states of

excitement. However in reality glass has some composition impurity's that absorb some of the radiation passing through. What also makes glass so popular in civil engineering is its chemical resistance to many aggressive substances, where also lies the secret of its durability [1.].

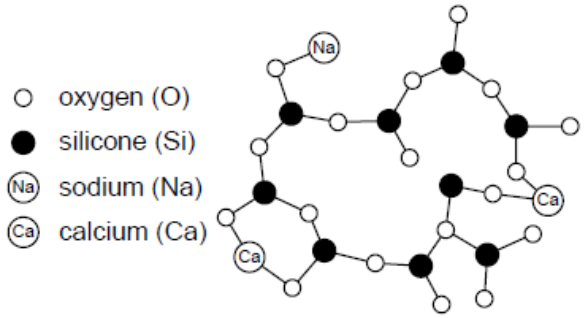

Figure 2.2 – Planar representation of the SLSG network [1.]

As previously stated, glass is a linear-elastic material, but that is only valid for a certain range of temperatures in which also lie the usual ambient temperatures. Its elastic properties, Young's modulus (*E*), are also dependent of the chemical composition the glass. In presence of high temperatures the value of *E* modulus drops until it is negligible around 600°C. While the E modulus diminishes the glass tends to behave as a liquid (around 500°C) and the binding forces diminish [5.].

The following table represents the main mechanical properties of float glass (which may vary from manufacturer to manufacturer) that will be used in the course of this master thesis.

Table 2.1 – Material properties of glass [1.]

Material	ρ [kg/m3]	E [GPa]	α_t [1 / °K]
Float glass	2.5E+03	70	9E-06

2.2.2 Strength

As all materials in civil engineering glass exhibits a tensile and a compressive strength, where the compressive strength is much higher than the tensile one and that is why defining the tensile strength during bending forces is very important. When talking about tensile strength of glass, there are two main principals to be distinguished. The first one is the theoretical strength and the second one is the actual strength.

What defines the theoretical tensile strength of glass is the covalent connection between its elements, which is a material constant and may reach 32GPa. This strength can never be achieved because of the many flaws, flaw types and flaw sizes present in the glass. This flaw dependency gives an enormous necessity to define the strength of glass. The different flaws (cracks) appear naturally in the processes of maintenance, transportation and construction, and are mainly responsible for the scattering of glass's actual strength, which is why it is not a material constant. Also the actual strength is very load type, load period and load rate dependent, that is to say that it's not constant trough time. The actual strength is around 50 to 100MPa.

2.2.3 Fracture Mechanics

The extreme homogeneity of glass along with the elevated strength of its covalent cohesive bonds is the cause of huge stress concentration in the microscopic region around crack tips. The crack propagation is thus very efficient, involving very little bulk dissipation and relatively efficient conversion of the mechanical energy into the surface energy required to create new fracture surfaces [2.].

Fracture mechanics describes the influence of the surface flaws, caused by the notch effect, and stress concentration on glass's tensile strength. There are three principal fracture modes (Figure 2.3) which can combine, forming more complex ones.

Mode I describes a fracture perpendicular to the crack surface tension, while Modes II and III describe fractures represented by the transverse and longitudinal shear stress respectively, however it is generally acknowledged to use only Mode I for tensile and bending stresses.

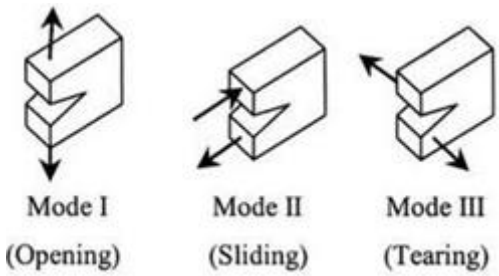

Figure 2.3 – Glass's main fracture modes [17.]

The stress intensity factor (K), which represents the elastic stress intensity near the crack tip, was introduced in order to characterize a material in terms of brittleness or fracture toughness.

As previously stated, only the fracture Mode I will be considered, and its stress intensity factor is given by the following equation for an idealized constant stress:

$$K_I = Y\sigma\sqrt{a\pi} \quad (1)$$

where Y is known as the geometry correction factor and it depends on the load type as to account for more realistic stress fields, the crack and specimen geometry and the proximity of the crack to the boundaries of the specimen; a is the flaws depth; σ is the stress on the tip of the flaw.

Therefore the instantaneous failure of a glass element occurs when the elastic stress intensity, K_I, is equal or higher than the critical stress intensity factor, K_{Ic}, and the stress on the flaws tip equals the critical stress. That is called the unstable crack growth. The equation can be also rewritten in order to quantify the critical depth of a crack for a constant stress.

2.2.4 Sub-critical Crack Growth

For stress intensity factors inferior to the critical stress intensity factor crack growth still occurs and is called the sub-critical crack growth and is a consequence of the stress corrosion. Stress corrosion, also known as "classical stress corrosion theory" [1.], involves a chemical reaction (Figure 2.4) between the water and the silica molecules at the tip of a crack. That is why stress corrosion practically doesn't occur in vacuum.

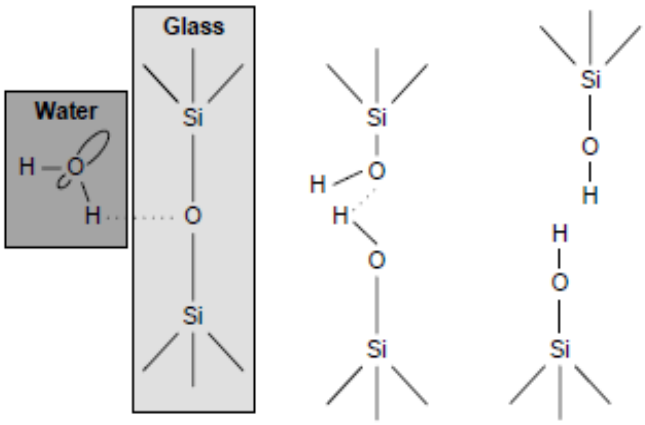

Figure 2.4 – Chemical (stress-corrosion) reaction between water and silica molecules [1.]

For the chemical reaction to occur there also needs to be a crack opening stress present which happens when the stress intensity factor exceeds the crack growth threshold K_{th}. The momentary strength of glass diminishes when the two before mentioned conditions are met.

In this condition the specimen can be loaded beneath its momentary strength, and still fail after the necessary time for the critical crack to grow.

The final consequence of sub-critical crack growth is fatigue. In order to determine glass's fatigue susceptibility crack velocity of the specimens is measured by monitoring the controlled growth of microscopic cracks. The next figure illustrates the relation between the crack velocity, *v*, and the stress intensity factor, K_I.

As mentioned before, sub-critical crack growth can only occur after exceeding the crack growth threshold.(Figure 2.5). Following that is the Region I that is governed by the velocity of the chemical reaction, and so, depends highly on the humidity. The Region III represents values of K_I which are very near the value of failure K_{Ic}, and where the chemical process ceases to occur. The explanation for this is as follows, the velocity in which the crack propagates reaches such magnitudes that the supply of water can't keep up with, making this region environment independent. In this region the specimen fails instantly, which is why the line is so steep. The two before mentioned regions are connected by an intermediary Region II, in which the chemical process is still valid, but has reached its limit; that is to say, the velocity of the particles of water reaching the tip of the crack is almost the same as the velocity of the chemical reaction.

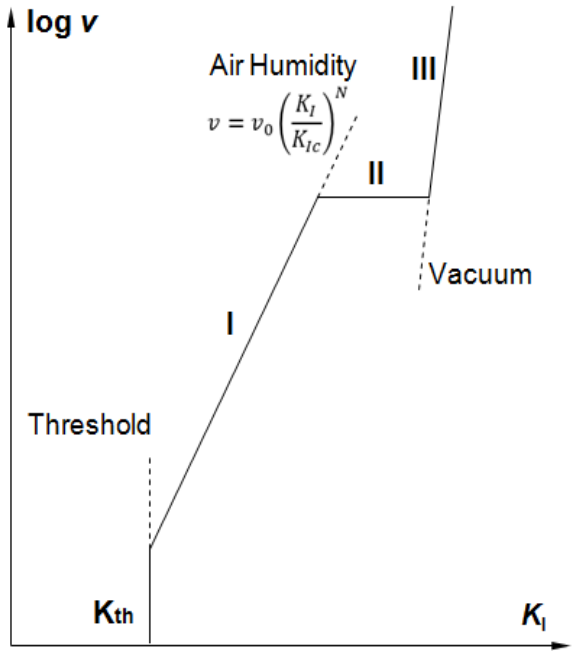

Figure 2.5 – Sub-critical crack growth development [20.]

Cracks in glass specimens grow for the greatest length of time in the Region I. Although the curve is divided into several regions, Region I is of primary interest in characterizing fatigue

behavior, since crack growth in this region is controlled by the rate of reaction of water with the glass [3.].

The behavior of crack propagation strongly depends on the environment, on the supply of water to be more specific. This is to say that in environments with higher concentration of water, the velocity of crack propagation achieved for the same stress intensity factor is higher (Figure 2.6).

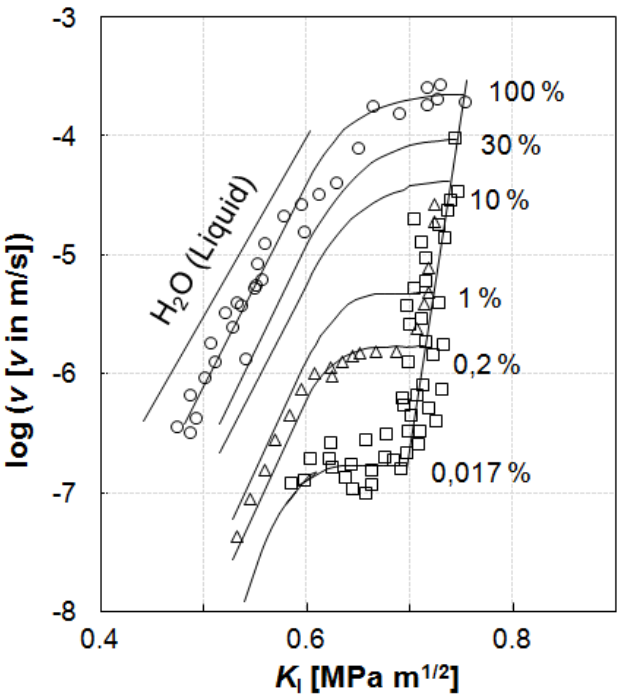

Figure 2.6 – Sub-critical crack growth development for different humidity [24.]

2.2.5 Fatigue Prediction

Fatigue occurs in some point of time after a loading period, be it static, dynamic or cyclic. For the first two loading cases there already exist suitable models for the theoretical determination of the life time prediction. Cyclic loads, however, have not yet been so extensively studied and as such the implementation of suitable models is yet to be tested.

Power law is an empirically derived law which is used to describe the glass's life time prediction and is used to describe the straight in the Region I, as it is of primary interest, of the sub-critical crack growth.

$$v = \frac{da}{dt} = AK_I{}^N \tag{2}$$

where A is the crack propagation constant and N is a material constant which is ambient dependent. A = 0,01 is commonly used as a standard value for room temperature and a humidity of 50%.

By substituting equation (1) in equation. (2) results:

$$da = AK_I{}^N = A(\sigma Y\sqrt{a})^N dt \tag{3}$$

For static and dynamic loads the empiric formula is directly derived by putting the equation (3) in order of σ^N and integrating the right side. Then by applying the respective circumstances (Figure 2.7) results equation (4) and equation (5), respectively for static and dynamic loading.

$$\sigma_{f,s} = \left(\frac{2}{(N-2)AY^N a_0{}^{(N-2)/2} t_f}\right)^{\frac{1}{N}} \tag{4}$$

$$\sigma_{f,d} = \left(\frac{2(N+1)}{(N-2)AY^N a_0{}^{(N-2)/2} t_f}\right)^{\frac{1}{N}} \tag{5}$$

where a_0 is the initial crack's depth and is a constant, t_f is the time of the failure and σ_f is the failure stress ant the time of the failure. By fixing the failure time one can obtain the failure stress and vice-versa.

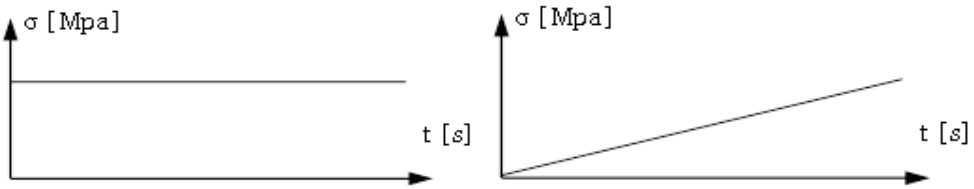

Figure 2.7 – Representation of static and dynamic stress development [24.]

For the cyclic fatigue an adjustment needs to be made before the formula can be applied, as it is not as well studied yet. So the approach used to define the critical stress is by considering that a cyclic load can be substituted by an equivalent static one equation (6). It is assumed that the equivalent static stress provokes the same crack growth as the cyclic stress, for the same time interval.

$$\int \sigma_{f,s}{}^{N} = \int (\zeta \sigma_{max})^{N} \tag{6}$$

where ζ is the area factor that describes the relationship between the equivalent static load and the maximum value of the cyclic load.

For a triangular loading function (Figure 2.8), as it is partially defined by a constant strain-rate, the $\zeta\sigma_{max}$ factor can be defined by equation. (4) in the following way:

$$\sigma_{f,s} = \zeta \sigma_{max} \tag{7}$$

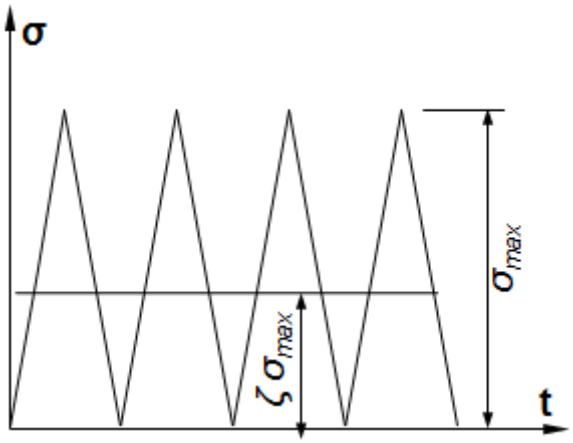

Figure 2.8 – Cyclic stress by considering an equivalent static stress [20.]

As the loading function is triangular σ_{max} can be replaced with $\sigma_{f,d}$ equation (5) in the equation (7). Then by solving it in order of the ζ factor it becomes obvious that it only depends of the crack velocity parameter N:

$$\zeta = \frac{\sigma_{f,s}}{\sigma_{f,d}} = \frac{1}{(N+1)^{1/N}} \tag{8}$$

2.2.6 Glass Strengthening

It is at the surface that glass contains the major flaws which are the most dangerous for its integrity. The flaws can only grow if exposed to tensile stress. Therefore it is good practice to strengthen glass, which consists in creating residual compressive stress near the surface and in turn not allowing the flaw to grow (Figure 2.9). Glass strengthening can be achieved by heat tempering and chemical tempering. The side effect of tempering is the appearance of tensile stress in the core of the glass. The flaws present in the glass's core are much smaller and therefore do not present any threat.

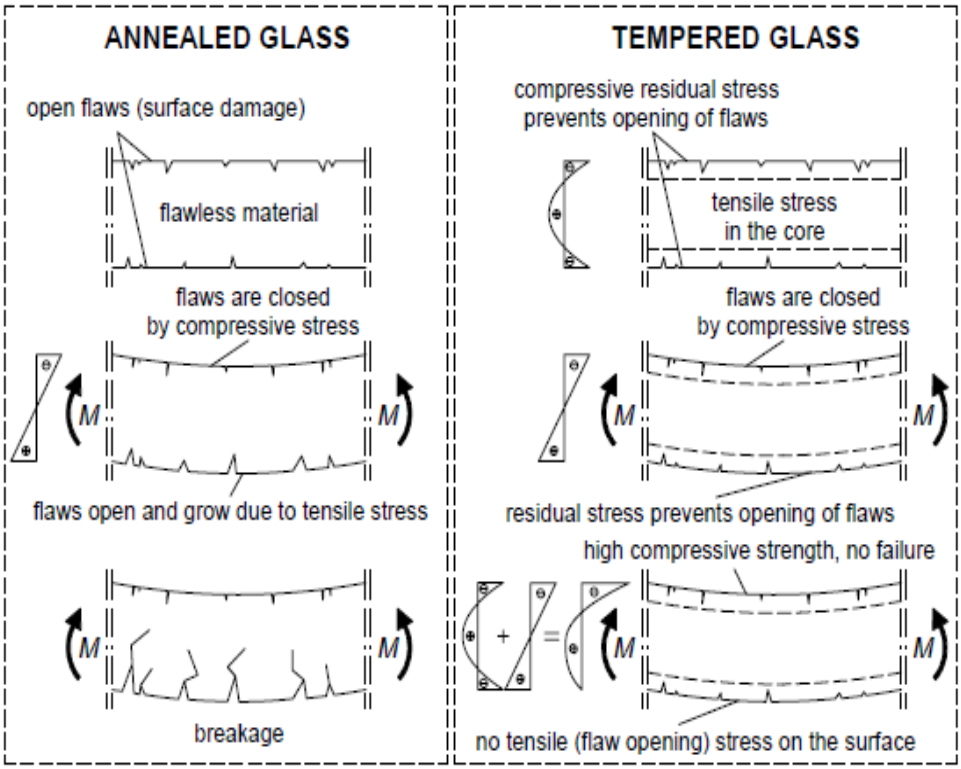

Figure 2.9 – Annealed (float) glass vs. tempered glass[1.]

2.2.6.1 Heat Tempering

Heat tempering [1.] consists of heating up the float glass to approximately 650°C and then rapidly cooling by jets of cold air at a controlled rate. The heat tempering can be done in two ways: by fully tempering or heat strengthening. What distinguishes the two types is the rate at which they were cooled down. Fully tempered glass is cooled down at a much higher rate than the heat strengthened glass and therefore presents higher residual compressive stress. This higher residual stress is due to the higher energy stored in the glass. The higher the energy stored, the smaller are the pieces when the glass breaks (Figure 2.10). The remaining short term post breakage capacity of glass depends on the size of the broken pieces: larger pieces bear against each other on an arch like effect; small pieces are less stable, with a less advantageous post breakage behavior. In the case of laminated glass, this leads to the so called wet towel effect.

Heat tempering has a peculiarity and that is the glass should be cut or drilled after tempering as working the heat tempered glass can easily cause it to shatter.

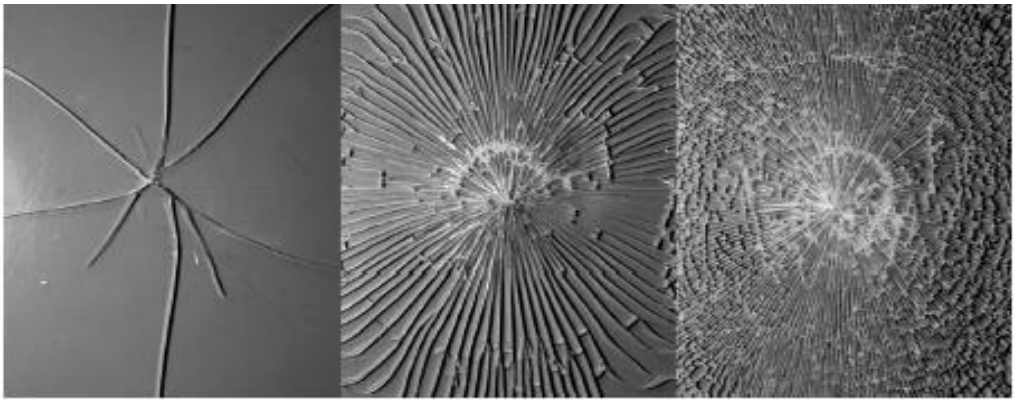

Figure 2.10 – Fracture patterns for float, heat strengthened and fully tempered glass, respectively [1.]

2.2.6.2 Chemical Tempering

As the name implies, chemical tempering is performed by altering the surface chemically and is performed by the ion-stuffing technique. The glass is slowly cooled in a salt bath of molten potassium, where the sodium ions of the glass are being substituted by the potassium ions. During this process a denser and therefore a stronger surface layer is created.

Chemical tempering has the advantage over heat tempering by being possible to cut or drill the glass, although at that point it loses all of the residual strength. It still has another huge disadvantage. The disadvantage is that the mobilized residual compressive strength doesn't go deep enough into the specimen giving way to crack tips being exposed to crack opening strength. And that is why it isn't usually used in structural applications, apart from special geometries where heat tempering cannot be used [1.].

2.3 Plastic Interlayer

Plastic interlayers are being commonly used in lamination because of their unique response to mechanical loads, and that is why it is important to study their physical and chemical properties. Also as they are peculiar materials which in some instances, behave as elastic solids and in others as viscous fluids it is important to study their temperature strain and strain rate behavior. This material behavior will be discussed further in this sub-chapter.

2.3.1 Polyvinyl Butyral (PVB)

The polyvinyl butyral (PVB) is the most common interlayer for the laminated glass used in vehicles and in architectural applications. It is a product of PVB resin, softeners and additives. Softeners are used because the mechanical properties of the resin, such as strength and elasticity, aren't high enough as to be used in a structural way. Additives are chosen so that certain properties such as cold failure temperature, water absorption capacity and adhesion to glass meet the requirements [12.].

The resin is produced in 3 stages [16.]: in the 1st stage raw materials are connected through catalysis and polymerization; in the 2nd stage occurs saponification; in the 3rd condensation in an acidic medium. The intermediate products are being weight-percentage controlled so the adhesion to glass's surface can be guaranteed.

The final product is obtained (Figure 2.11) after mixing PVB resin, plasticizer and addictive's in the extruder until a homogenous mass emerges. Then follows extrusion, through a bride nozzle in where "constant and precise thickness" can be achieved, and treatment of the surfaces so that they would not adhere to anything else before the lamination. Finally the interlayer is cut in designed pieces, cooled down and then stored.

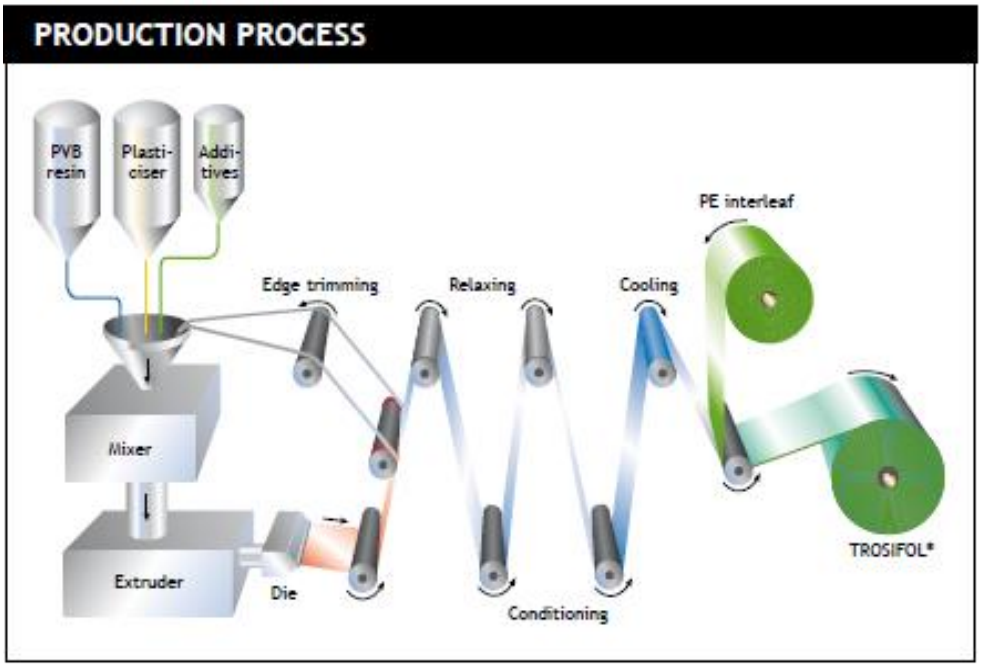

Figure 2.11 – Production of the PVB interlayer [16.]

2.3.2 Material Properties of PVB

"PVB is an amorphous thermoplastic material with highly temperature dependent behavior" [18.]. It doesn't have an orderly molecular structure. The macromolecules are partially entangled and don't present any network between them. It is in those partially entangled places that some low intermolecular forces arise enabling a reasonable deformation behavior through energy input, by temperature increase or deformation, within a certain temperature range [12.].

The principal material properties of PVB which clarify as to why it is so commonly used in laminated glass are its good adhesion and strong binding properties, its optical clarity, its toughness and flexibility.

The material properties for the PVB are assumed to be the following:

Table 2.2 – Elastic properties of PVB at 20°C

Material	Model	K [GPa]	G [GPa]	ν
PVB	Barredo	2,00	0,427	0,3908
	Duser	2,00	0,471	0,46

PVB's mechanical characteristics are substantially influenced by the strain-rate, level of strain, ageing and temperature of the specimen and quantity of water present at the time of testing. These factors can significantly reduce the interlayer's adhesion and bond strength capacities.

2.3.3 Small-Strain Behavior

In presence of small-strain (<0.1%) PVB responds at first with a linear-elastic behavior, making it a perfect fit to apply the Hooke's law. This first response is due to the deformation performed by the entanglement's being only of shifting position. The moment a certain strain limit is exceeded, the relaxation process initiates and the entanglements stretch and redirect along the direction of deformation. This leads to a reduction of the resulting stress, assuming that the applied strain is constant. This second response is what defines the viscoelastic behavior of PVB and its combination with the first response is described as the linear viscoelastic behavior.

For a linear viscoelastic behavior, in the presence of strain, the linear-elastic response provides a spontaneous limited reversible deformation, and then an unlimited time dependent viscous deformation initiates. When the stress gets relieved the material tends to revert itself to the original state.

In presence of small-strain an idealized model called the generalized Maxwell model for tensile strain, which represents the complex time-dependent mechanisms present in the linear viscoelastic material and the stress relaxation behavior, is applied. Although the model is accurate for most polymers, it has a limitation: it cannot predict creep accurately.

The Maxwell Model (Figure 2.12) is composed of an elevated number of elements which are connected in parallel. Those elements go by the name of Maxwell elements and are divided in spring and dumpers. The springs, whose stiffness is represented by the shear modulus *G*, represent the elastic behavior, whereas the dumper with a certain dumping constant represents the viscous behavior. The model is closed with a linear elastic spring with a shear modulus equaling G_∞, which is the limit of the time dependent shear modulus *G(t)*. The single spring represents the linear elastic behavior of the material at an advanced time t_∞, and describes the regression of the viscous deformation. At time *t=0* the shear modulus is a sum of all the elastic sprigs shear modules.

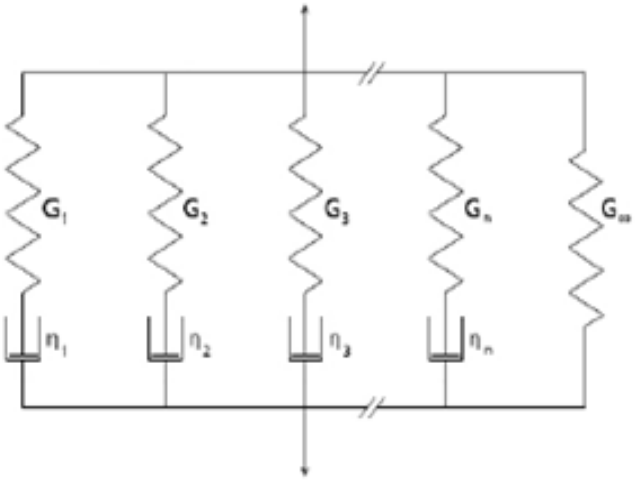

Figure 2.12 – Generalized Maxwell model [13.]

The time dependent behavior of PVB is divided in to two parts: shear relaxation and volumetric relaxation. The time dependent shear relaxation behavior of the Maxwell model was considered by the means of a prony series equation (9). A prony series serves to estimate the frequency, amplitude, phase and damping components of a curve. The volumetric relaxation is relatively unchanged through time [10.] thus it was neglected.

$$G(t) = G_0 \left(\alpha_\infty + \sum_{i=1}^{n} \alpha_i e^{-\frac{t}{\tau_i}}\right) \quad (9)$$

were τ_i is the reduced time and α is the prony series parameter for the dampers and elastic springs respectively. The two most well know prony series are the Barredo (Table 2.3) and the Duser (Table 2.4) prony series. For the FEM models only the Barredo values were applied unless stated otherwise.

Table 2.3 – Barredo prony series parameters at a reference temperature of 20°C

τ_i	3.09E-07	3.08E-06	3.07E-05	3.07E-04	3.06E-03	3.05E-02	3.04E-01
α_i	1.51E-01	1.91E-01	1.41E-01	1.84E-01	1.39E-01	1.22E-01	5.40E-02
τ_i	3.03E+00	3.02E+01	3.02E+02	3.01E+03	3.00E+04	2.99E+05	
α_i	1.37E-02	2.11E-03	9.46E-04	9.65E-05	2.75E-04	1.54E-04	

Table 2.4 – Duser prony series parameters at a reference temperature of 20°C

τ_i	3,26E-11	4,95E-09	7,24E-08	9,86E-06	2,81E-03	1,64E-01
α_i	1,61E-01	7,88E-02	2,91E-01	7,12E-02	2,69E-01	8,96E-02
τ_i	2,26E+00	3,54E+01	9,37E+03	6,41E+05	4,13E+07	
α_i	3,02E-02	7,61E-03	9,63E-04	4,06E-04	6,14E-04	

Beyond a certain strain(>200%), the linear viscoelastic material behavior can no longer be assumed and the material crosses over to the large-strain domain. For large-strain the behavior of the material is vastly different since PVB presents a great time dependency and the available large-strain material approach doesn't account for it and also, since in this thesis only the small-strain behavior is of interest, large-strain models won't be discussed.

2.3.4 Temperature-Time Dependence

The shear modulus of a polymer is considerably sensitive to temperature changes. At low temperatures, below the transition temperature (T_G), PVB presents a glassy-like constitution; it behaves as an undercooled liquid and presents a rigid material behavior. With the decreasing of the temperature increases the rigidity of the material until it reaches the glassy state. This state is located beneath the glass transition T_G which ranges from 10°C to 23°C for PVB [12.]. At temperatures above T_G an inverse constitutuin occurs, which ranges from leathery to liquidy.Strain-rate dependence is invercely proportional to the temperature dependence, that is, the higher the temperature and or the lover the strain-rete the lower is the value of the shear modulus and vice versa.

The temperature can be considered through the Williams-Landell-Ferry (WLF) shift function (equation (10)), which is an empirical equation associated with time-temperature superposition. As its name indicates, it shifts results horizontally. For known properties at a reference temperature, it is used to predict the temperature-dependent properties of linear viscoelastic materials.

$$\log_{10}(\alpha_T) = -\frac{C_1 \cdot (T - T_0)}{C_2 + T - T_0} \tag{10}$$

where α_T is the shift function, C_1 and C_2 are material constants, T and T_0 are the ambient and references temperatures respectively.

Table 2.5 – WLF function parameters for Barredo and Duser

WLF	C_1	C_2	T_0
Barredo	49.806	328,46	20
Duser	21	91,1	20

2.4 Laminated Glass

Laminated glass is a composite of two or more sheets of glass, which are glued together by a polymer interlayer (PVB or other adhesives of high strength and stiffness), thus creating a discrete connection between the sheets and guarantying an adequate strength and stiffness of the laminate. For the PVB to be used as an interlayer in laminated glass it must present at least a tensile strength of 20 MPa and a technical elongation break of 250%. The most common process to produce laminate glass is autoclaving at a temperature of approximately 140°C and at a pressure of approximately of 1400KPa [1.]. The heat and an appropriate pressure ensure that there are no air bubbles enclosed between the glass and the interlayer. It is stipulated that to achieve a good adhesion, the PVB interlayer is required to present a humidity of [0.4; 0.5]% [7.]. And that is why when the interlayer is stored after its production, it is wrapped in a water proof film.

The mechanical behavior PVB can also be divided in small and large-strain. The small-strain behavior is of the essence to determine the bending behavior of uncracked laminates, whereas the large-strain behavior is of the essence in cracked laminates while being able to undergo large tensile extensions and providing a connection between the fragments.

The small-strain behavior of the laminate is limited to below the breaking of the glass sheets. However when in the presence of bending strain, which is the predominant mode of deformation, the PVB interlayer lies in a neutral zone making it improbable that it comes even

near its small-strain. In this strain range the interlayer's main function is to transfer horizontal shear force as well as keep the glass sheets at a distance from each other. The amount of shear stress that PVB can transfer between the glass sheets is temperature and strain rate dependent. That is to say, at low strain-rate or high temperatures, as the stiffness of the PVB is low, the amount of shear stress that can be transferred between the sheets is low, and the laminate tends to behave as two independent sheets (Figure 2.13 a)). At high strain-rate or low temperature, as the stiffness of PVB is high, the amount of shear stress that can be transferred between the sheets is high, and the laminate tends to behave as an equivalent monolithic glass sheet (Figure 2.13 c)) with the sum thickness of the glass sheets.

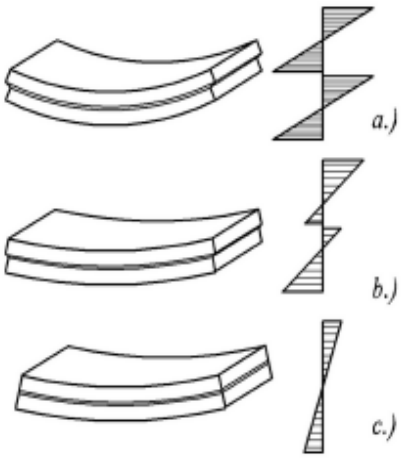

Figure 2.13 – Bending behavior of laminates [21.]

As monolithic glass doesn't present any ductility, so its behavior after failure is simple, it disintegrates. But for the laminates the bending failure behavior consists of 3 stages: 1st one of the glass sheets cracks, then follows a rapid fragmentation of both glass sheets, and at the end occurs extension until failure of the interlayer. During this extension period a certain remaining load bearing capacity is obtained as the glass fragments adhere to the PVB. That is only possible because the fragments lock in place and adhere to the interlayer. This makes the material safer and more secure, by minimizing the risk of injury and/or property damage during severe events.

2.5 Coaxial Double Ring (CDR)

In order to sufficiently understand a material's behavior, tests and testing procedures are indispensable. The test that will be described in this sub-chapter and further implemented in laboratory conditions is called coaxial double ring (CDR) test and is used as a proxy for cyclic, dynamic and static loading. In this test an equibiaxial stress field ($\sigma_1=\sigma_2$) is obtained.

CDR is especially useful to determine experimentally the bending strength of specimens because the edges of the specimen don't have any influence on its strength which is advantageous because the cracks often initiate from there. CDR consists of two rings, one is the load ring and the other one is the support ring. The stress originated by the load ring in the area enclosed by it is uniform and represents the maximum value (Figure 2.14); therefore the probability of the specimen failing because of the biggest surface defect within that area is high.

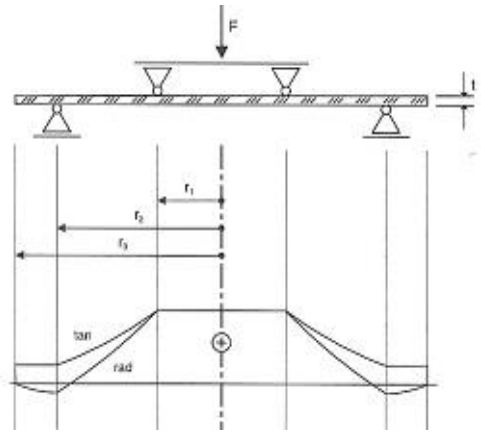

Figure 2.14 – CDR, qualitative representation of the radial and tangential stress on [5.]

Characteristic glass's strength is typically used for glass design and is represented by the following values: 45MPa and 22,5MPa, which respectively represent the short and long term failure stresses for the 5% of the specimens when in presence of a stress-rate of 2MPa/s while subjected to a CDR force controlled tests [1.].

The norms EN 1288-5 and EN 1288-2 (Table 2.6) describe the standards in order to perform the CDR tests on not pre-damaged glass. The dimensions of the rings chosen were the following: r1=40mm and r2=80mm (r1=30, r2=60 for the float glass specimens). Although the dimensions for the rings and for the specimen don't match with the ones presented in the norms it doesn't matter, as the specimen will be pre-damaged in order for the induced flaws to be critical, making the norms obsolete.

Table 2.6 – CDR test geometries in European standards [1.]

Designation	Standard	Loading ring radius (mm)	Reaction ring radius (mm)	Tested area* (mm^2)	Specimen edge length (mm)
EN CDR R45	EN 1288-5 [116]	9	45	254	100 (±2)
EN CDR R400	EN 1288-2 [114]	300 ± 1	400 ± 1	240 000†	1 000 (±4)

3 SIMULATIONS: PRELIMINARY STUDIES

3.1 Introduction

In this chapter some of the statements made in the previous one were analyzed through numerical modeling and other preliminary studies did took place, by resorting to a sophisticated finite element software called *ANSYS Workbench*, commonly used to verify the experimental data of 2D/3D objects.

3.2 Structural Model

The models were made in order to represent the geometry of the specimens (sub-chapter 4.3) and the conditions of the CDR test (sub-chapter 2.6), where the inner and the outer circles respectively represent the load and the support rings configured as illustrated in the Figures 3.1 and 3.2.

For the modeling, weak springs and large deformations were activated to respectively eliminate the horizontal displacement and to consider the second order effects. For the temperature dependent viscoelastic behavior of PVB an environmental temperature of 21,5°C was used.

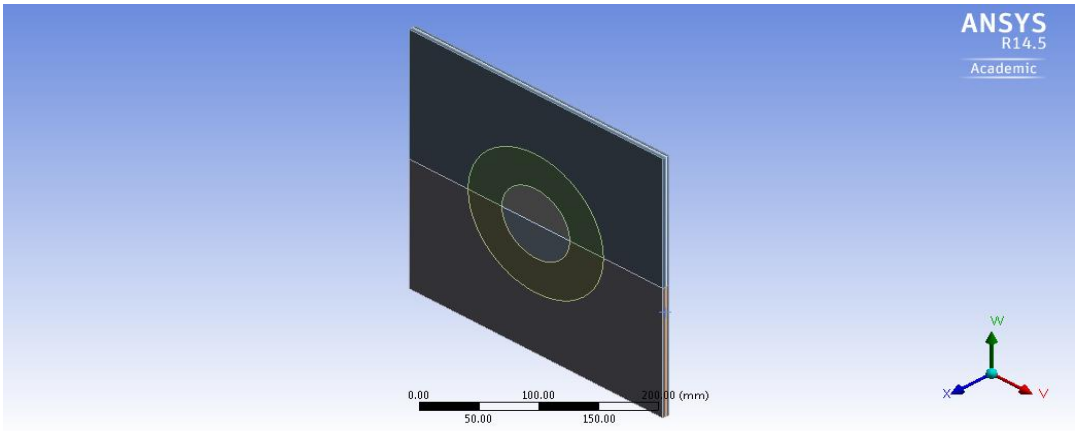

Figure 3.1 – Model of the laminate (300 x 300)

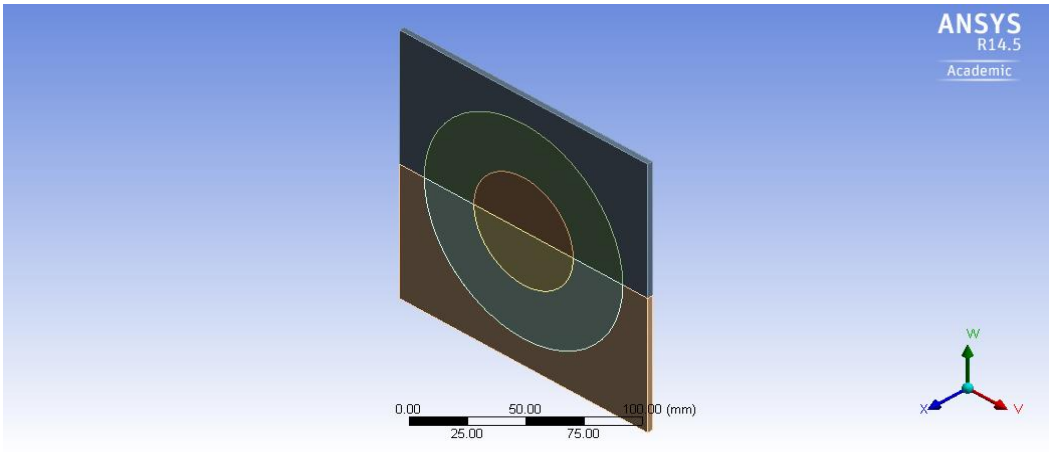

Figure 3.2 – Model of the float glass (150 x 150)

3.3 Mesh Study

In order to obtain a sufficiently precise analysis and not to turn the calculations too heavy a mesh study was performed prior to the calculations. The purpose of this study is to identify the minimum mesh discretization for the planar elements, the surface and the thickness, from which no significant accuracy improvement may be achieved.

As mentioned before, the area enclosed by the loading ring presents a uniform maximum stress and therefore has a bigger influence on the results and as such it needs to present a finer mesh. The area between the loading ring and the supporting ring is of lesser importance, and the area outside of the supporting ring is of small or no importance.
The mesh study is performed for glass specimen with the surface dimensions of 300mm x 300mm (further the same mesh is assumed for float glass specimen with the surface dimensions of 150mm x 150mm) and was divided in 2 stages:

- Defining the mesh of the surface of the float glass

- Defining the number of elements to represent the thickness of the glass sheets integrating the laminate (for the PVB's thickness, only one element was considered as to avoid elements that are too thin).

For the 1st stage the study was performed for a range of loads and the resulting deformation in the middle of the tensile surface of the modeled float glass specimen was recorded. So for the 1st iteration it was decided to have quite a coarse mesh sizing (Figures 3.3 and 3.4). The

analysis led to the conclusion that the sizing of the mesh doesn't has any practical influence on the results (Figure 3.5). Figures 3.6 and 3.7 illustrate the sizing of the adopted mesh in the 1st stage, and Figures 3.8 and 3.9 illustrate the sizing of the adopted mesh for the smaller float glass specimen.

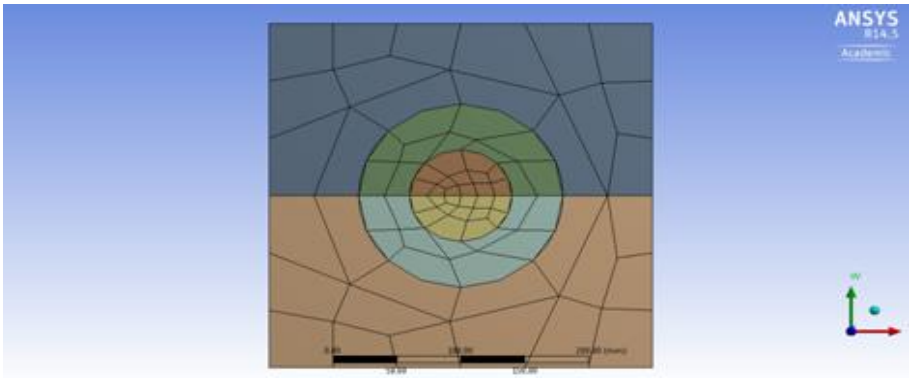

Figure 3.3 – Initial planar mesh sizing of the float glass sheet (300mm x 300mm)

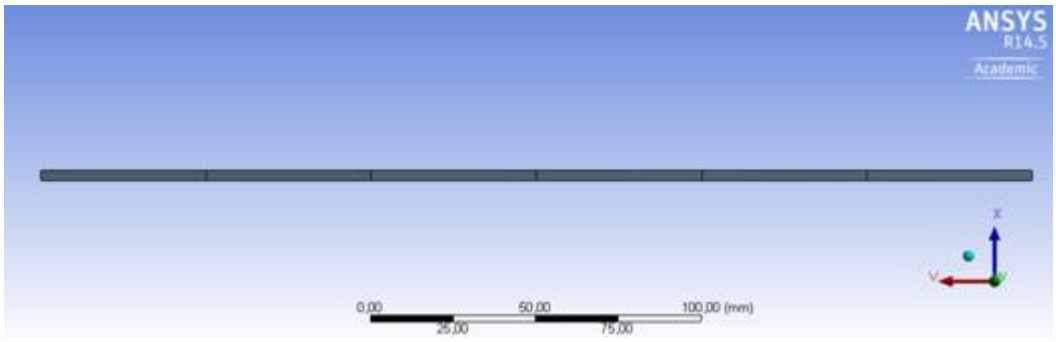

Figure 3.4 – Initial thickness mesh sizing of the float glass sheet (300mm x 300mm)

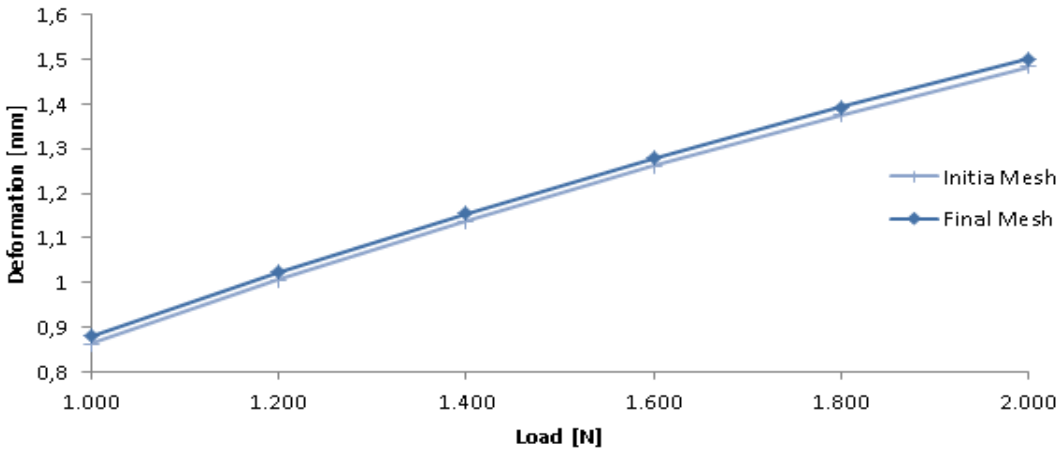

Figure 3.5 – Comparison between the initial and final mesh (1st stage)

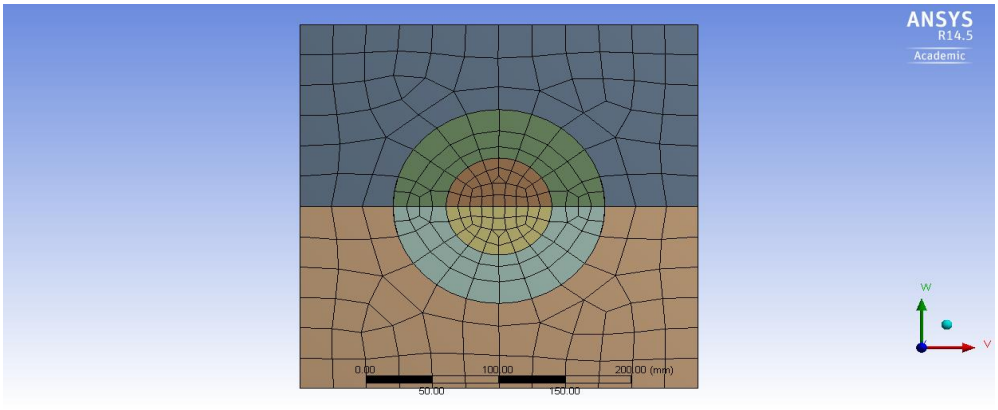

Figure 3.6 – Final planar mesh sizing for float glass sheet (300mm x 300mm)

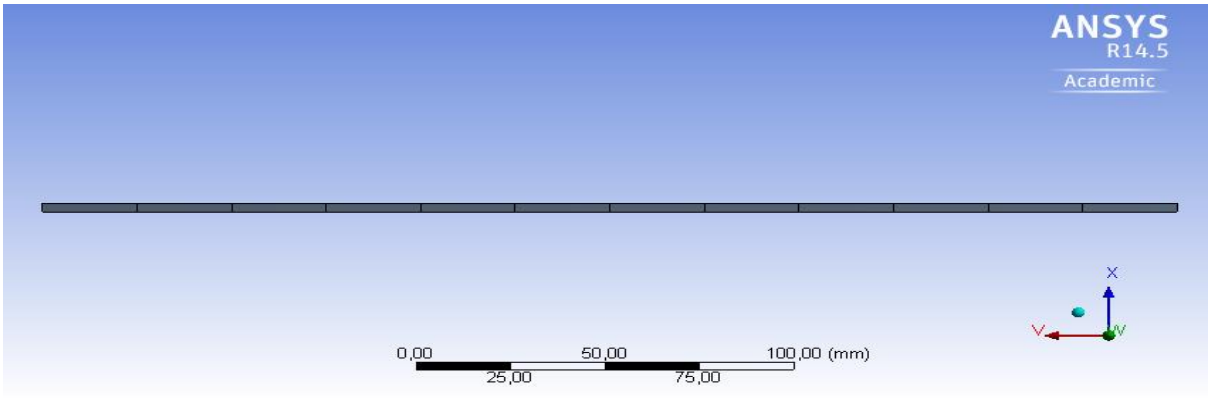

Figure 3.7 – Final thickness mesh sizing of the float glass sheet (300mm x 300mm)

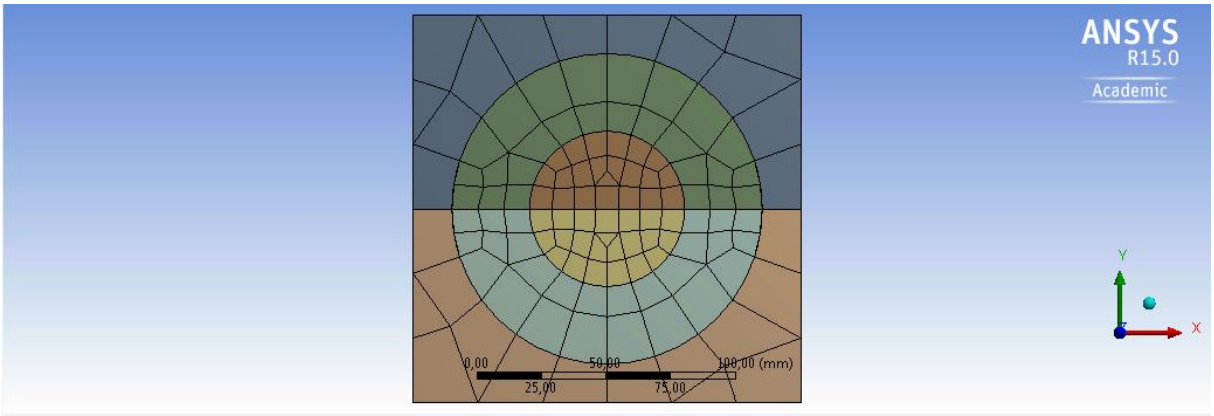

Figure 3.8 – Final planar mesh sizing for float glass specimen (150mm x 150mm)

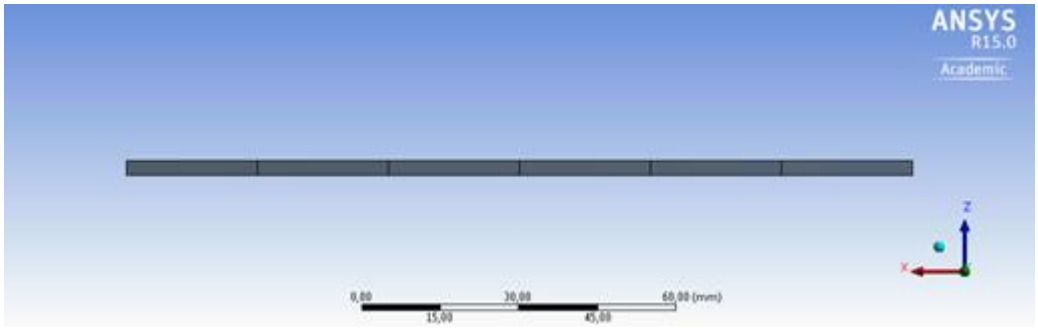

Figure 3.9 – Final thickness mesh sizing of the float glass specimen (150mm x 150mm)

For the 2st stage the study was performed for a fixed displacement of 0,25mm and the resulting stress, along a diagonal of the tensile surface of the modeled laminate, was recorded. The analysis was performed by varying the number of elements representing the glass sheets (Figures 3.10 to 3.11) which led to the conclusion that the number of elements also doesn't has any practical influence on the results (Figures 3.12). The Assumed number of elements was assumed to be 1 (Figure 3.11).

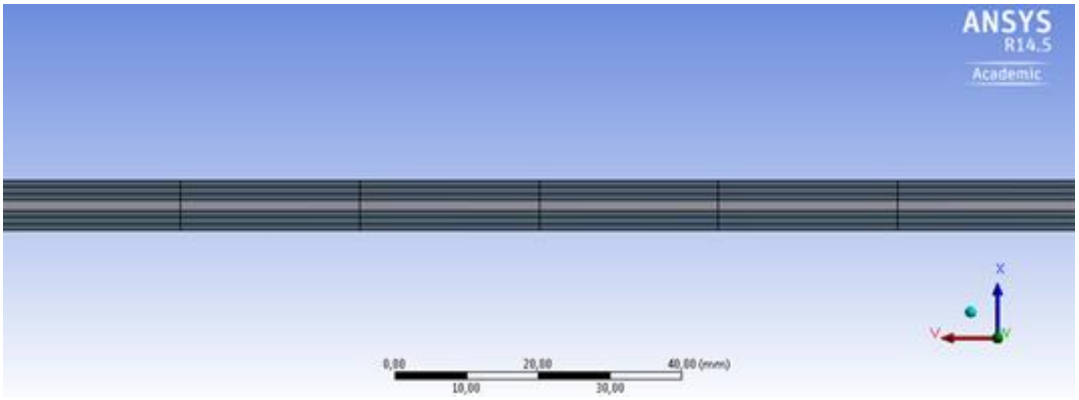

Figure 3.10 – 3 elements for glass's thickness

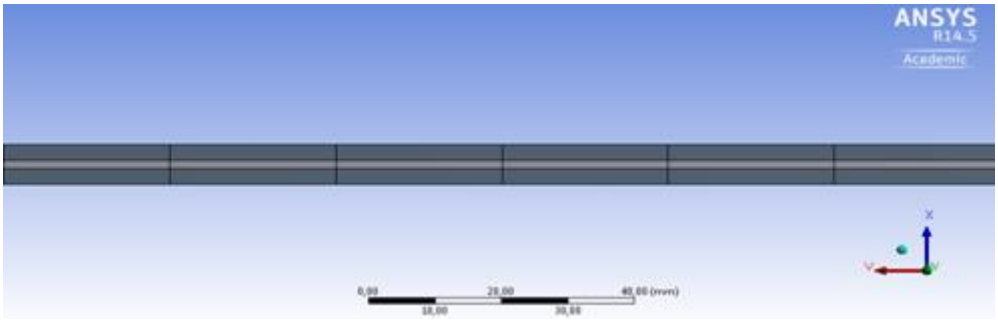

Figure 3.11 – 1 element for glass's thickness

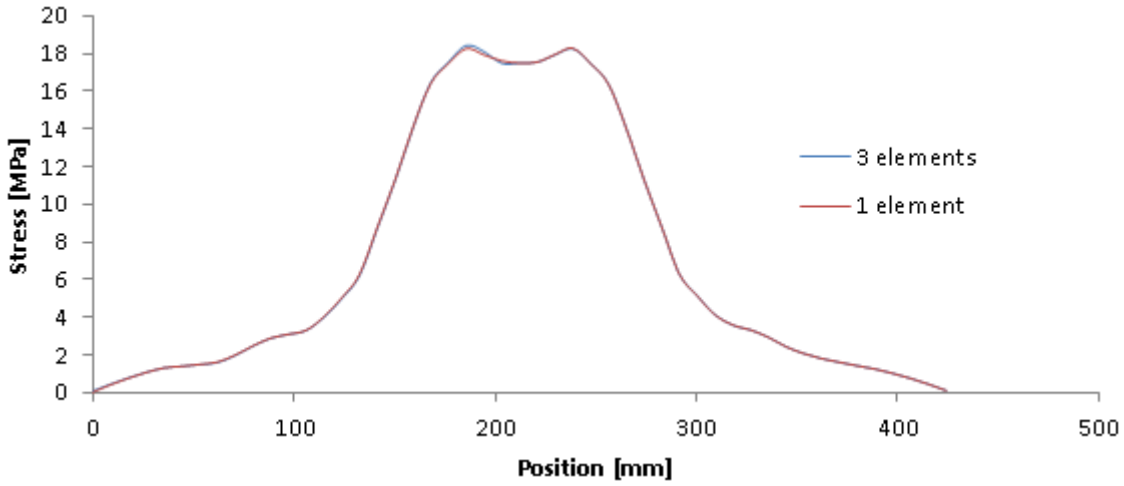

Figure 3.12 – 2nd stage mesh study on the laminate

Figure 3.12 demonstrates that in presence of CDR bending tests the stress development along the area enclosed by the load ring can be considered uniform and the maximum, and the edges don't have any influence on the specimen's strength as the stress development is negligible.

Figures 3.13 and 3.14 demonstrate the modeled behavior of the tensile surface of a laminate in terms of stress and deformation for the adopted mesh, when simulating CDR bending test conditions with a fixed displacement of 0,25mm. Further simulations of laminates in this chapter are performed for the same CDR bending test conditions

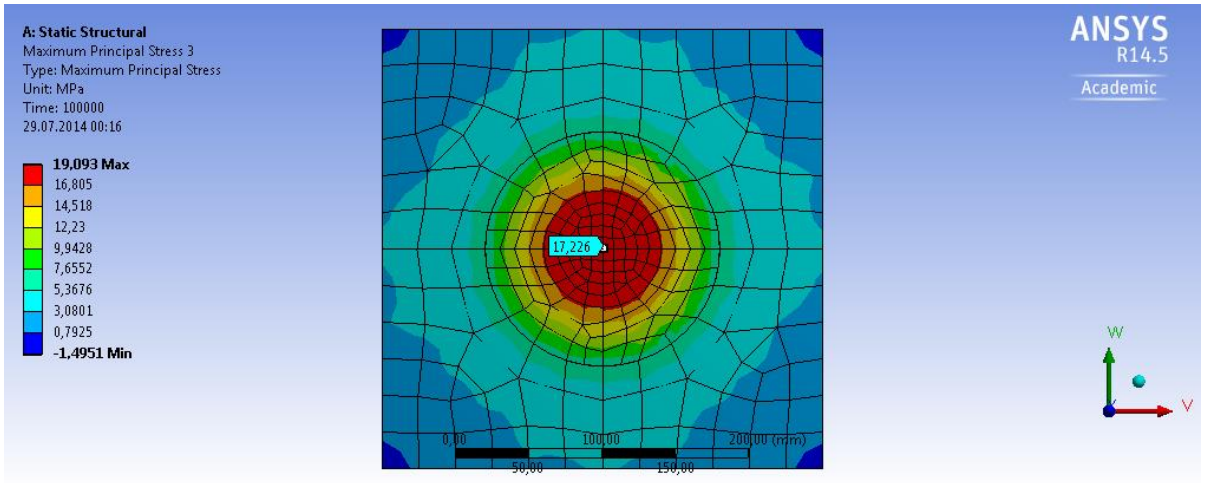

Figure 3.13 – Development of the principal stress on laminates

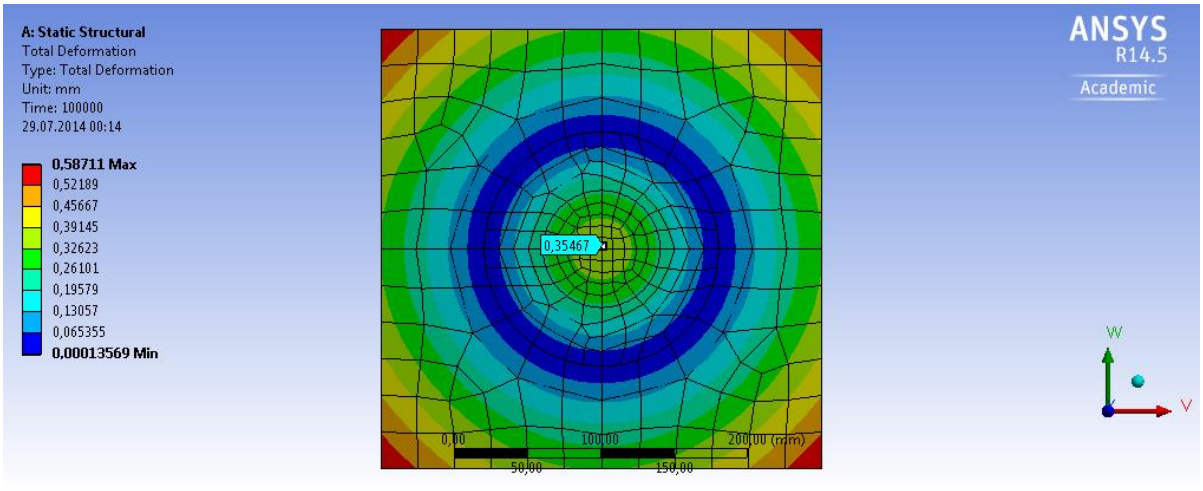

Figure 3.14 – Development of the total deformation on laminates

3.4 PVB's Time Dependent Simulation

As mentioned before a laminate can behave as a monolithic sheet with the sum thickness of the glass sheets for short-term loads (or low temperatures) or as two independent sheets for long-term loads(or high temperature), due to the interference of the plastic interlayer. This FEM study (Figure 3.15) is performed in order to verify that statement

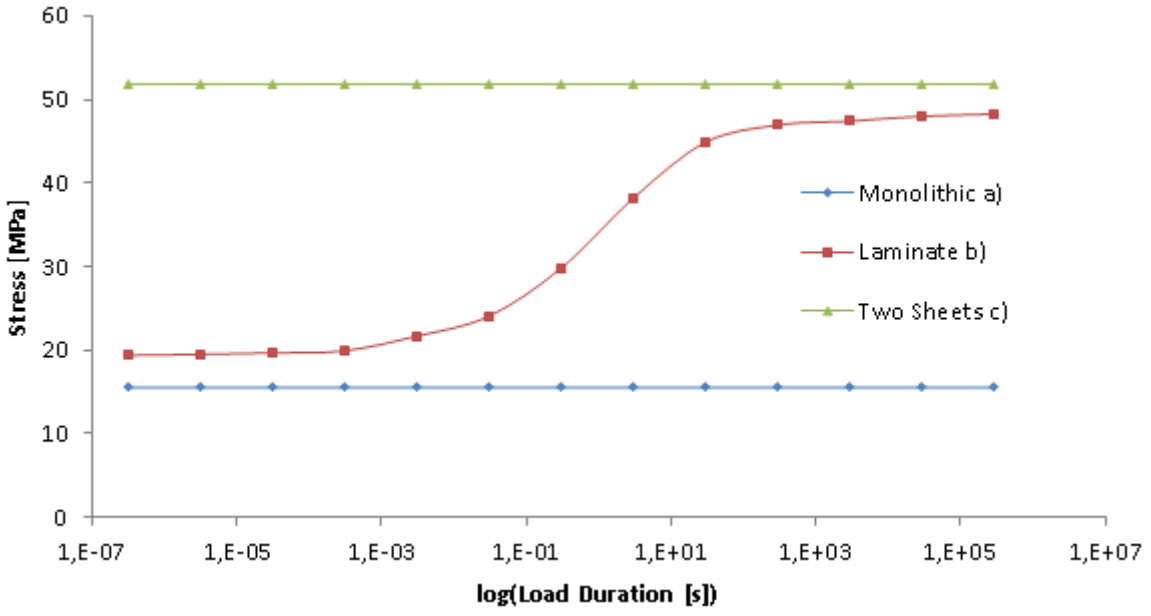

Figure 3.15 – Behavior of a laminate

The difference in strength (stress) between the monolithic sheet and the two independent sheets lies in the moment of inertia, which is respectively: $I=bh^3$ and $I \approx 2b(h/2)^3/12=bh^3/48$. As the stress is inversely proportional to the moment of inertia it means that the stress that develops in the monolithic sheet is lower than the one that develops in the two independent sheets in presence of the same conditions. The existence of PVB puts the inertia and therefore also the strength of the laminate in between of the two extremes.

3.5 PVB's Elastic and Viscoelastic Simulations

Values of the Shear modulus of PVB can be extracted from a respective prony series, characterizing the viscoelastic behavior of the material, for specific points in time. Afterwards the obtained values can be inputted in the material properties of PVB (by assuming only the elastic behavior) in the FEM model of the laminate. Theoretically, the results returned from this FEM model should be compatible with the ones returned from the FEM model which also incorporates the viscoelastic behavior of PVB.

As the two FEM models, for the Barredo approach didn't seem to agree with each other, the Duser approach was also utilized for comparison (Figure 3.16). As it is, no conclusions could be derived from this study, as one cannot just say that the prony series isn't a good feet to define the elastic behavior of PVB without the knowledge of how such a prony series is created. For further simulations of the behavior of PVB it was decided to utilize the Duser's approach.

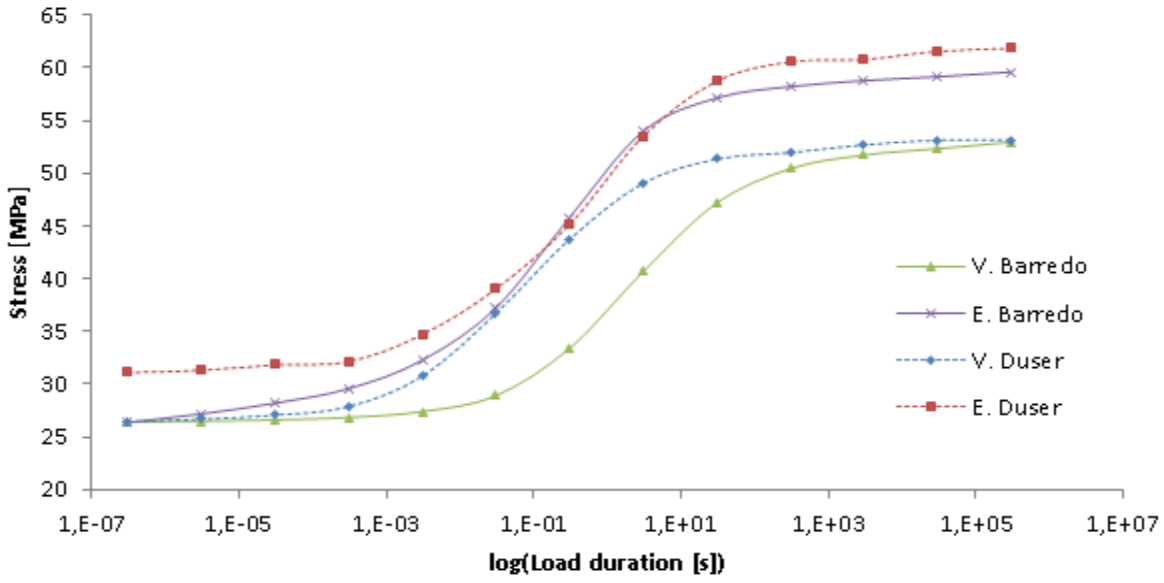

Figure 3.16 – Elastic vs. viscoelastic behavior of PVB for Barredo and Duser

4 EXPERIMENTAL PROCEDURES

4.1 Introduction

The main objective of this thesis is to determine the bending behavior of laminates in presence of cyclic loading. For that two things are of essence: on one hand to experimentally determine the material behavior of the glass, the interlayer and the laminate as a whole, by measuring the strain for the small-strain tests (which serves to describe the PVB's behavior) and by measuring the failure time for large-strain tests (which serves to describe float glass's and laminate's fatigue behavior); and on the other hand, to obtain data for the validation of the FEM. But before they can be performed a set of laboratory proceedings need to be defined and implemented.

4.2 Specimens

The ordered specimens were laminates (Figures 4.1 to 4.2) composed of two sheets of float glass with 3mm of thickness each and a PVB interlayer with 1.52mm of thickness. The planar dimensions of the specimens where 300mm x 300mm, as it was the easiest way for the manufacturer to cut and laminate. The laminate had its thickness purposefully chosen for the PVB interlayer to present an elevated volumetric influence on the whole. Float glass specimens of the same material were additionally ordered with its dimensions: 300mm x 300mm x3mm, those than were cut in 4 pieces each (Figures 4.3 to 4.4).

As one cannot guarantee that the ordered specimens present the requested dimensions, measurements needed to be performed. The measurements were only focused on the specimen’s thickness, as its variation has relatively more influence than the variation of the other two dimensions.

Upon arrival the laminate and float glass specimens where randomly selected, and their thickness was inspected, and as expected, they did not have the exact measures as ordered. By measuring the float glass specimens the average thickness was determined to be 2.89mm. By measuring the laminate’s thickness, 7.24mm, and then subtracting the measured float glass’s thickness, an average thickness of the interlayer was determined to be 1.46mm. All further numerical models contain the average measured thickness of the elements.

Figure 4.1 – Surface of the laminate (300 x 300)

Figure 4.2 – Thickness of the laminate

Figure 4.3 – Surface of the float glass (150 x 150)

Figure 4.4 – Thickness of the float glass

4.3 Experimental Setup

The CDR test was performed through the testing machine *Z050* (Figure 4.5) with electromechanical drive from the manufacturer *ZwickRoell*. The maximum compression force and velocity of the machine are 50kN and 600mm/min respectively. The test can be force or path controlled.

Figure 4.5 – Testing machine Z050 [5.]

The required test setup consists of the CDR rings (Figure 4.6) which are connected to the machine by cylinders. In order to avoid the propagation of bending moment the load ring is not fixed to the machine, but has an indirect contact through the intermediary that is a sphere which simulates a hinge.

Figure 4.6 – CDR rings (r = 40, r2 = 80) and sphere [5.]

The specimen is centered on the support ring and then the load ring with the sphere is positioned on top of it. The top cylinder goes down until it gets in contact with the sphere, by pressing it, on top of the load ring which needs to be adjusted per hand. The force with which the upper cylinder is pressing the loading ring should not exceed 150N, or else the software won't let the test start. The final setup, before a testing can begin looks like the following Figure 4.7.

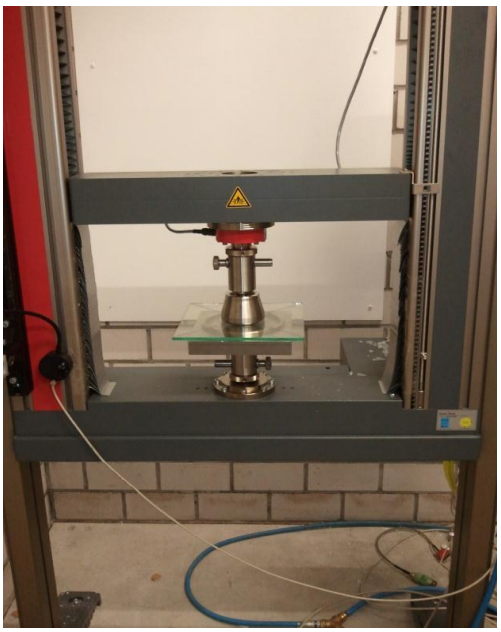

Figure 4.7 – Final setup with a laminate for the CDR bending test [5.]

As mentioned before, the fluctuation of the environmental conditions may greatly affect the results of the tests and that is why they need to be set and kept constant through the whole period of the tests. For that measure specific equipment were used, such as a humidifier, a dehumidifier and an air conditioner. With this equipment limits for the temperature and humidity were respectively set to be [21, 22]°C and [45, 50]%.

4.4 Induced Flaw

As previously stated, surface's flaws in glass present highly dispersed characteristics, and that is why the glass's strength is not relatively constant, but a huge dispersion of values. The strength's dispersion may lead to a failure time, when subjected to loading, of a few days or, take a very long period of time. So in order to potentiate the efficiency of the test it is prudent to induce superficial damage in form of small standard indentations (Figures 4.8 to 4.9). The indentations are supposed to be way bigger than the flaws that the specimens initially

presented in order for the specimen to fail through the induced flaw and not through any other pre-existing one, which reduces the dispersion of the glass's strength and the consecutive failure time. Two indentations were applied in order to further ensure that one of them is critical.

Figure 4.8 – 1Induced flaws (100 x magnified)

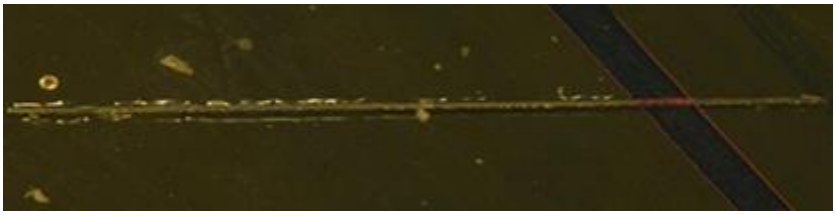

Figure 4.9 – Induced flaw (200 x magnified)

By observing the fracture pattern of a specimens it's easy to identify whether it failed because of one of the induced flaws or because of a pre-existing one. For that purpose on the back (compressive side) of the float glass specimens, additionally, an adhesive tape was applied in order for the specimen to be in a relative good condition after failure, that is, not to shatter in small pieces after being tested so the fracture pattern can be observed. In case any specimen reaches failure through another flaw it means that something went wrong, and that the specimen should be excluded from the study.

The flaw can be induced by means of a glass cutter, a sand paper, a laser, some acid, a diamond or others. The chosen means was the Konicher Diamond with an opening angle of 120° (as the 60° diamond was too damaged) which presents a lesser spread of the results [13.].

The two induced flaws were performed, in the center of the specimen, parallel to the contour of the specimens and to each other (with a distance of 2mm between them), by the *Universal Surface Tester (UST 1000)* (Figure 4.10). The specimen was marked with a cross, so that it would be easier to center the specimen on the *UST 1000*, on the compressive surface as to avoid any chemical reactions between the induced flaw and the ink. The place to perform the

indentations was purposely chosen to be in the middle of the specimen so, they can experience the maximum uniformed stress when in presence of the CDR bending test.

Figure 4.10 – UST 1000 [20.]

Before the flaw can be applied the following preparations need to be done: first the specimen is put centrally on a surface where by the means of tubes connected to holes in the surface is applied suction, immobilizing the specimen; then the tip of the diamond needs to be put at the right height as to touch the specimen but not to produce any excessive force on it; last but not least, after fulfilling the before mentioned requirements, the force with which the machine applies the indentation (which reflects its depth) and its length are defined and the flaw is induced. The length was decided to be 2mm, as increasing it doesn't has much impact (Figure 4.11). After the application of the indentation the specimen was rested for 15min and then tested immediately.

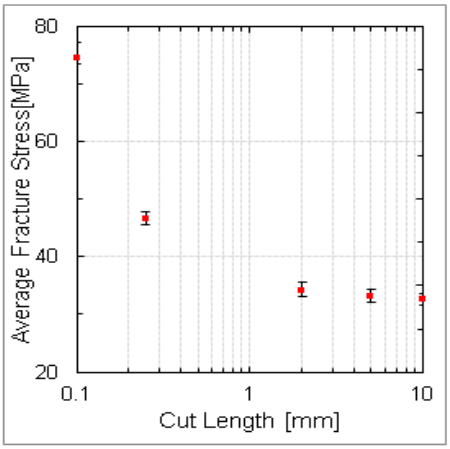

Figure 4.11 – Indentation's length importance for the specimens strength [24.]

4.4.1 Short Term Failure Load

As mentioned before, the objective of the induced flaws is to create conditions for the specimen to fail at the short term failure stress. That is why it is important to discover the load responsible for such a stress. In order to define that load a FEM static model for the float glass, for a range of forces, was performed. From the regression line (Figure 4.12) a load of 800N was withdrawn.

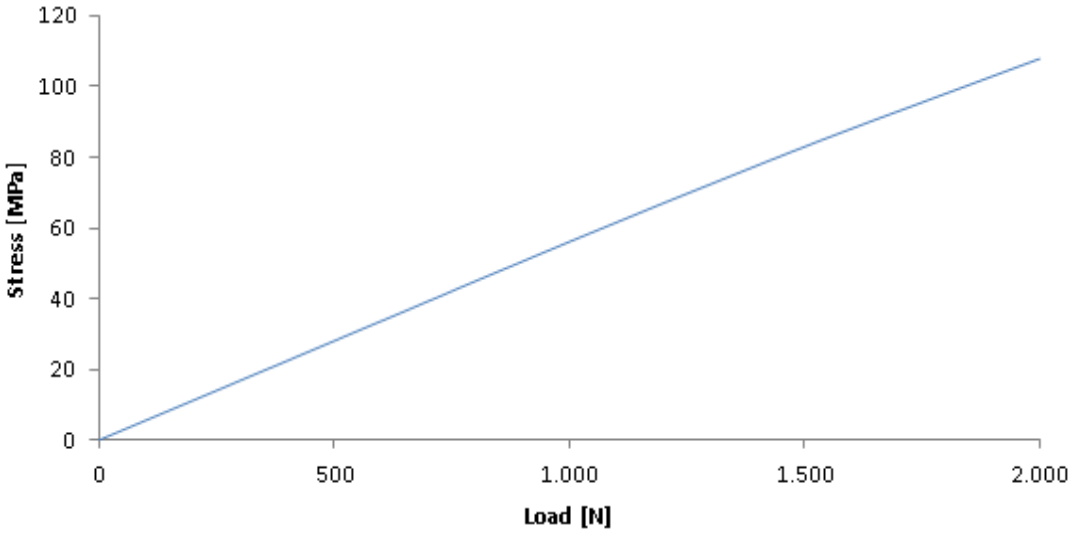

Figure 4.12 – FEM, load vs stress

4.4.2 Indentation Force

After discovering the value of the load which causes the short-term failure stress, follows the definition of the depth of the indentation that becomes critical in presence of that load. A simple approach for that is to define a indentation force, which reflects the desired depth. As such, flaws for different forces were induced on float glass, then the damaged specimens were tested. The tests were performed in a dynamic way with a stress-rate of 2MPa/s for different values of indentation force until failure. As the machine works with force units instead of stress units, force-rate was defined to be 35,56N/s. After evaluating a linear regression line for the experimental data (Figure 4.13), a value of 435mN originated for the indentation force.

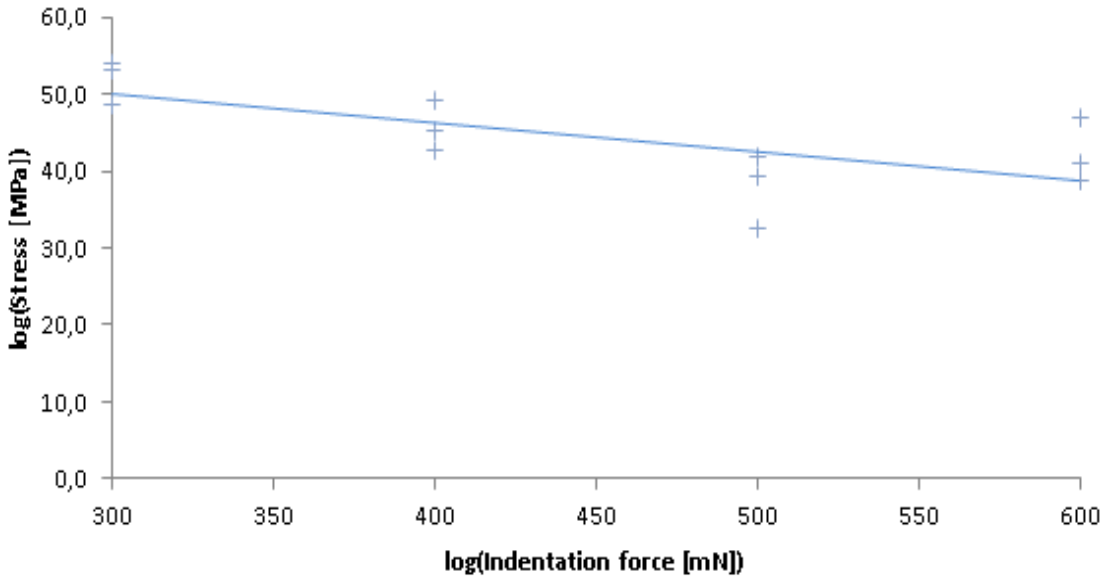

Figure 4.13 – Experimental, Indentation force vs Stress

4.4.3 Crack Velocity Parameter N

The crack velocity parameter *N* is a dimensionless value defined to be used in the glass's fracture strength prediction. It is greatly influenced by the glass's chemical composition, the environmental conditions and the load-rate (stress-rate). The stress-rates for which tests were performed are indicated in the Table 4.1.

N is derived from the dynamic fatigue of float glass and then further implemented in static and cyclic numerical predictions of laminated glass. Although *N* varies from load type to load type, it is not so significant that would make it imprudent to implement the derived value in other load type predictions. It is defined by plotting a regression line of log stress-rate vs. log failure stress (Figure 4.14).

Table 4.1 – Applied stress-rate

Stress-rate [Mpa/s]				
20	2	0,2	0,02	0,002

The slope of the regression line serves to directly define *N* via equation (11). From the regression line a slope of 0,0814 was extracted and the respective value of *N* was calculated to be 11,28.

$$Slope = \frac{1}{(N+1)} \tag{11}$$

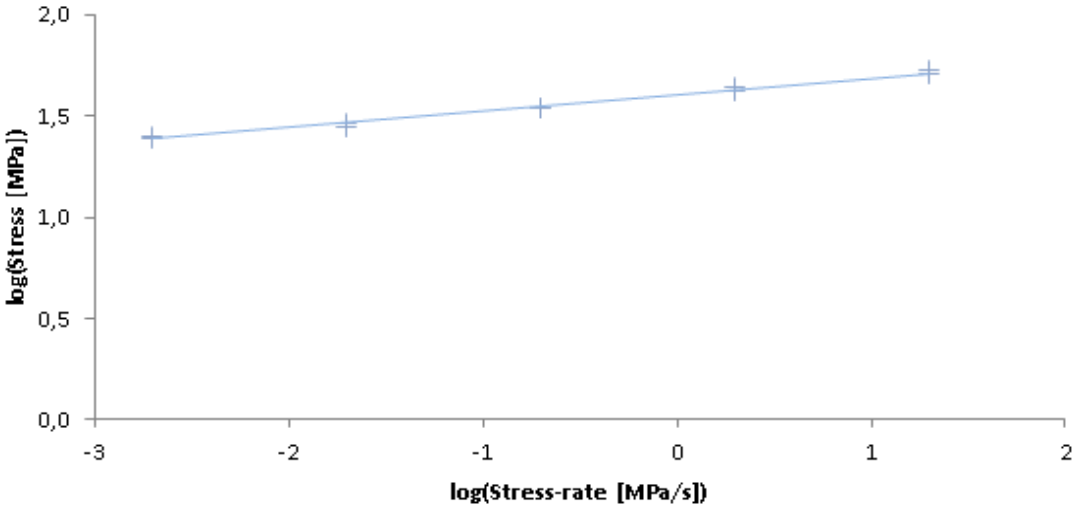

Figure 4.14 – Log stress-rate vs. log failure stress

4.5 Installation of DMS

The "Dehnungmessstreifen" (DMS) is a strain gauge chip used in order to measure the strain response of a specimen when in presence of loading and via equation (12) the respective stress can be calculated. The ship can only execute the intended task if the measured data is faultlessly transmitted to it, which requires an excellent connection. For that matter the chip was tightly glued to the surface which would experience tensile stress in the CDR bending test (Figures 4.15). Also the positioning of the chip was specially chosen to be in the center of the surface for the same reasons that the lad to the induced flaws being applied in the center.

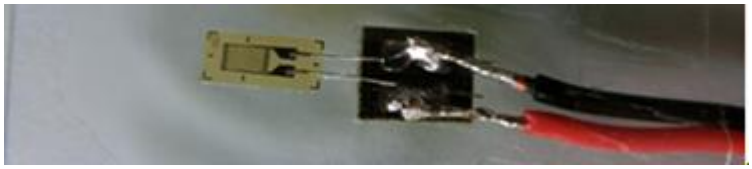

Figure 4.15 – DMS gauge chip

The DMS chip present in the specimen measures a one directional strain (ε) on the surface of the glass, which can be mathematically converted into global stress via the one directional strain and the Poisson coefficient ν of the glass sheets:

$$\sigma = \varepsilon * E/(1-v) \tag{12}$$

5 RESULTS AND ANALYSIS

5.1 Small-Strain Tests

Small-strain tests were performed on laminates for path controlled conditions. Those tests were performed on laminates, which presented DMS gauge chips in order to measure the obtained strain. Strain measurements were performed for static and cyclic loads. The objective of these measurements is to identify the behavior of the PVB interlayer present in the laminate. The other objective of these tests was to calibrate the testing conditions used for large-strain tests.

5.1.1 Static Strain Measurements

In order to determine the displacement with which the static path controlled test should be performed, that is, for it not to cause failure of the specimen, a numerical analysis was performed on a viscoelastic model (Figure 5.1). The objective was to identify a displacement which won't result in the long term failure stress of 22,5MPa. So the obtained displacement was of 0,25mm which caused a long term stress of 17,57MPa.

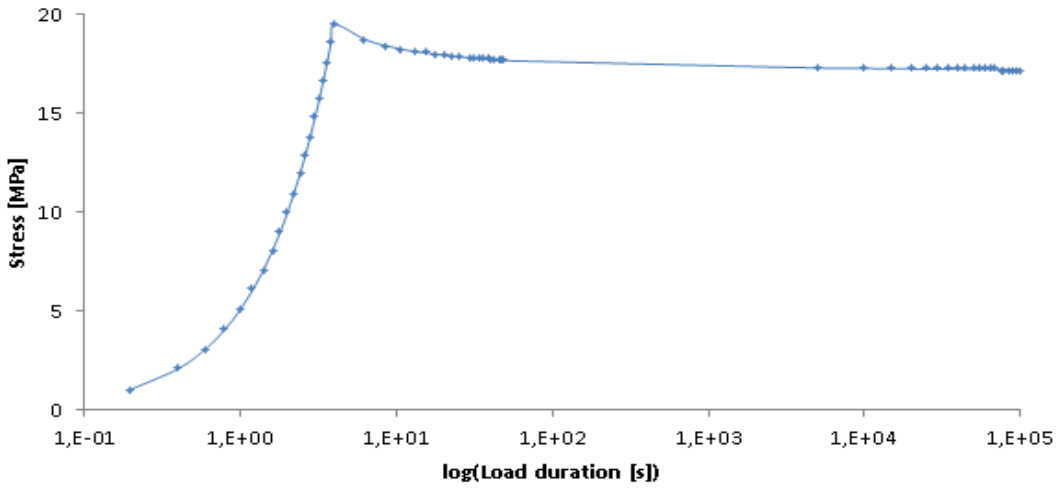

Figure 5.1 – FEM model, stress through time

The static path controlled test (Figure 5.2) was thus performed through the movement of the loading ring for a displacement of 0,25mm, with a constant rate until 4s, and then was held constant until around a time limit of 100000s. After evaluating the results it was concluded that the load needed to maintain the displacement constant diminishes through time after reaching the peak of 727N at 4s.This behavior for a path controlled test is due to the creep effect associated with the viscoelastic properties of the PVB interlayer. The load response needed to maintain the deformation tends to stabilize around the value of 528N.

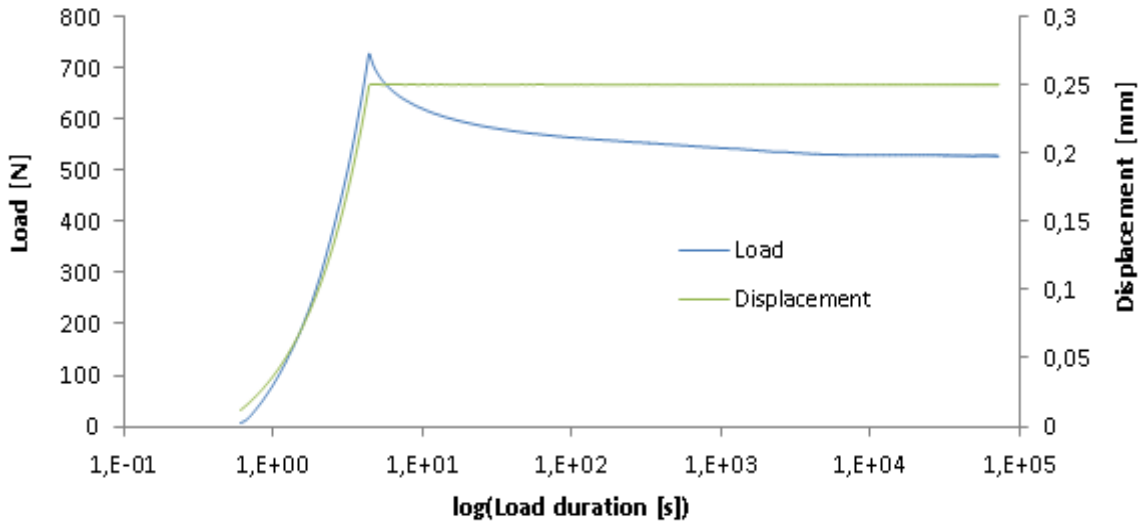

Figure 5.2 – Path through time and the respective load

5.1.1.1 Tests vs Viscoelastic Model

A comparison between the FEM viscoelastic model and the experimental data was made. The FEM viscoelastic model presents higher values of stress than what was obtained from the experimental data (Figure 5.3). That is because the real material properties of the PVB interlayer used in the laminates are unknown. So in order to obtain a more consistent, with the experimental data, FEM model, it would be prudent to experimentally determine PVB's material properties.

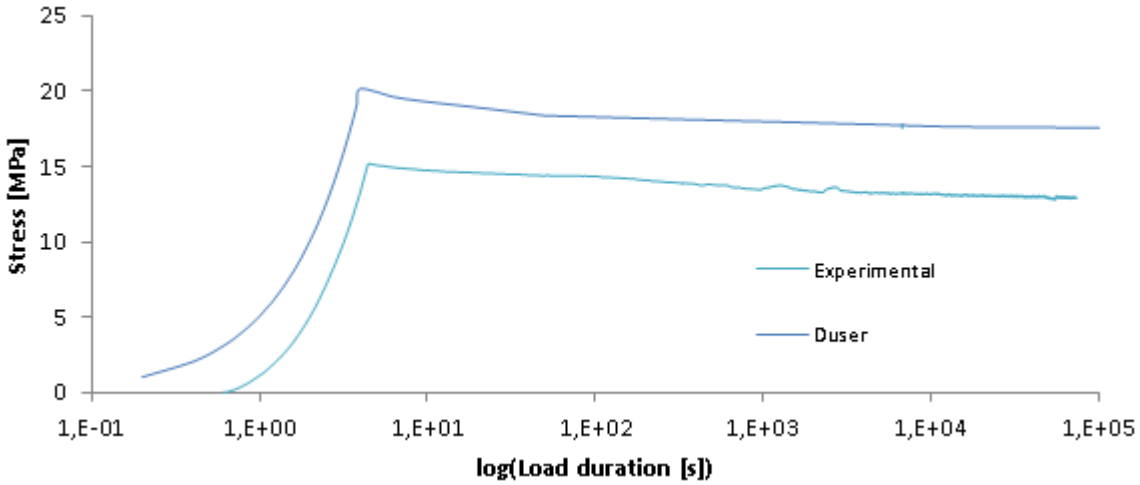

Figure 5.3 – Viscoelastic FEM model vs experimental data

5.1.1.2 Tests vs Elastic Model

Through an iterative procedure were studied the values of the shear modulus (Figure 5.4) needed to be inputted in the elastic model in order to reproduce a few points of the experimental data (Figure 5.2). It was done by matching the path and the force for those points, by means of adjusting the shear modulus in the elastic FEM model. Afterwards the stress obtained from the FEM model and the stress obtained from the experiments where compared (Figure 5.5).

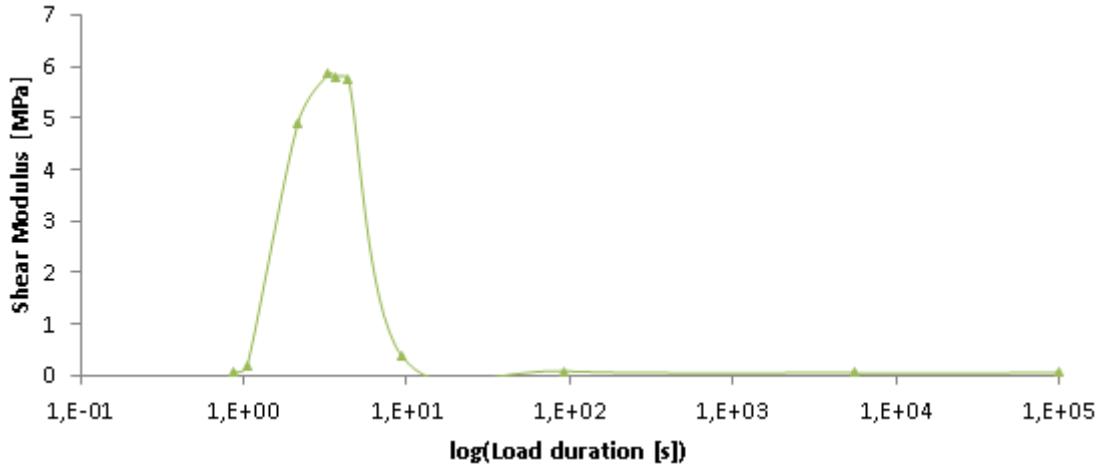

Figure 5.4 – Shear modulus for the elastic FEM model

The values for the FEM elastic model are also higher than the ones obtained through experimental data, though lower than the ones obtained from the FEM viscoelastic model (as could be expected while observing the Figure 3.17) and therefore are closer to the experimental data. That is why hence fort only the FEM elastic model is going to be considered.

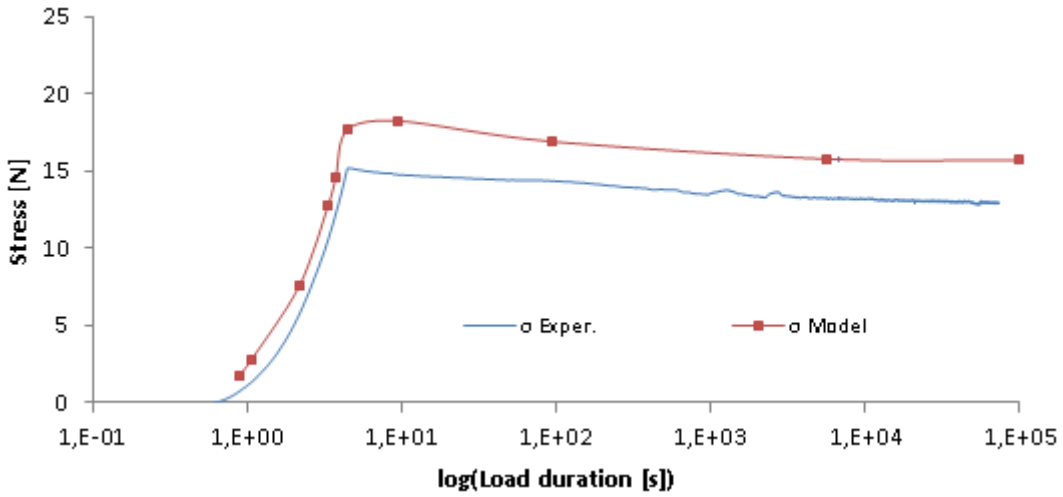

Figure 5.5 – Elastic FEM model vs. experimental data

5.1.2 Cyclic Strain Measurements

The cyclic path controlled test (Figure 5.6) was performed with the initial conditions of the static path controlled tests until 4s, and then a simple triangular path function was performed with maximum and minimum path amplitudes of 0,25mm and 0,04mm (the minimum path amplitude was different from zero in order to make sure that the loading ring and the specimen don't separate at a giving instant, and therefore avoiding impact during testing) respectively for a frequency of 0,535Hz. This test was performed until a period of 100000s.

The laminates behavior shows a brief initial decrease in the maximum response, to which follows a constant one, therefore the following figure exemplifies the behavior only for the first 120s. The cyclic behavior is quite different from the observed for static loading. That is, it doesn’t present the substantial long term decrease in the response. This constant behavior is due to the minimum path amplitude that is not high enough, resulting in quite a low static load component which almost doesn't influence the stress responses. Also in between cycles PVB experiences a long enough resting period as the frequency is low, and therefore recovers its material properties.

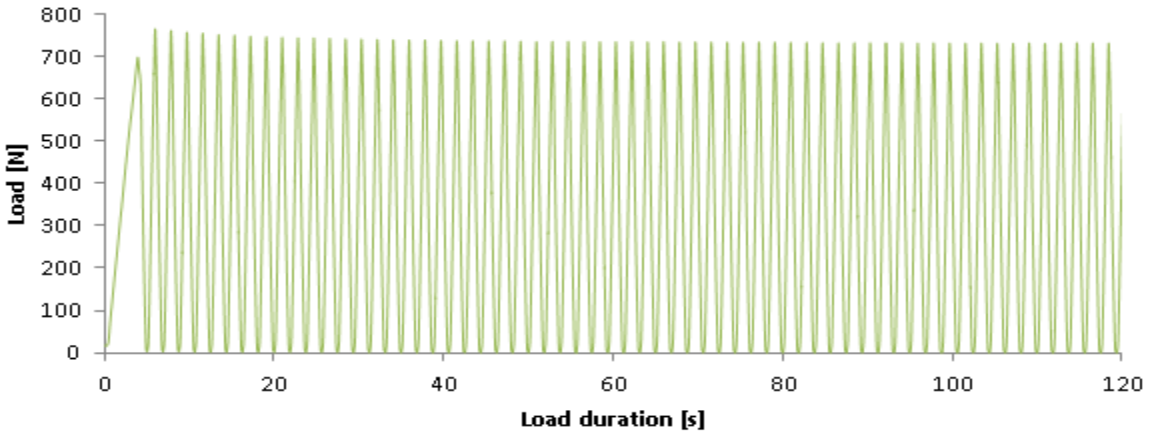

Figure 5.6 – Experimental load response through time

5.1.2.1 Viscoelastic Model

The FEM viscoelastic model presents higher values (Figure 5.6) of load response than what was obtained from the experimental data. The negative values of load response indicate that the minimum path isn't high enough when performed by the FEM model. The FEM model, similarly to the experimental data, presents a brief initial decrease in the maximum response, to which follows a constant one.

Also in this case in order to obtain a more consistent, with the experimental data, FEM model, it would be prudent to experimentally determine PVB's real material properties.

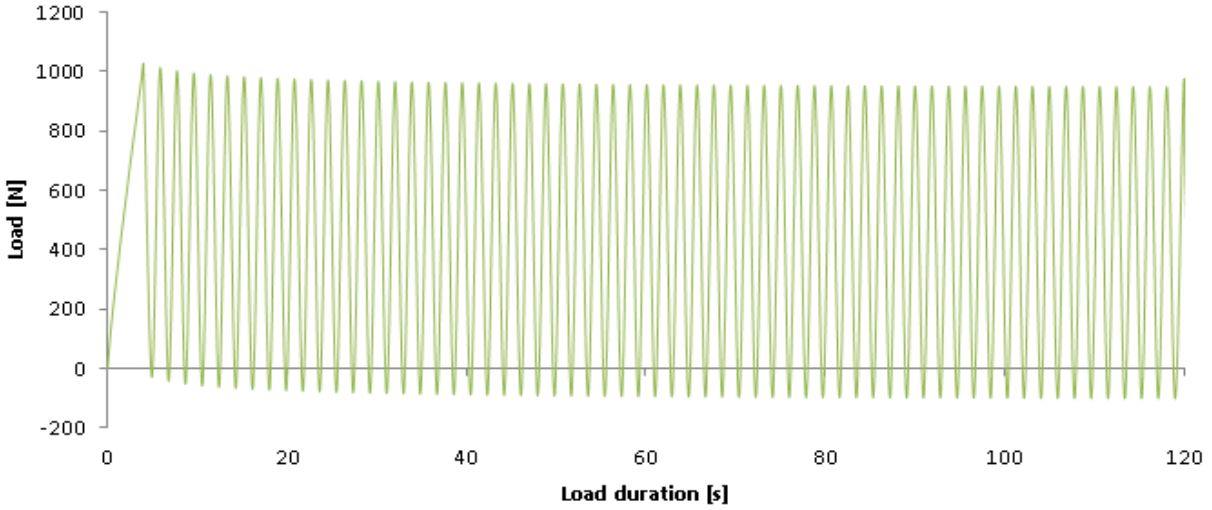

Figure 5.7 – FEM model load response through time

5.1.2.2 Cyclic Strain Measurements vs. Frequencies

Cyclic path controlled tests were also performed for other frequencies in order to perceive if the constant behavior replicates and if the maximum response amplitude changes. The cyclic tests were alternately performed on two specimens, where they were loaded alternately for the same set of frequencies (Table 5.1), until a time instant of 120s. Between the consecutive testing of the specimen, for different frequencies, a resting period of 5min occurred so the PVB interlayer has enough time to recover its material properties. Next are presented examples for the load response and the path conditions during testing for one of the specimen for the following frequencies: 0,117Hz and 0,144Hz (Figures 5.8 to 5.11).

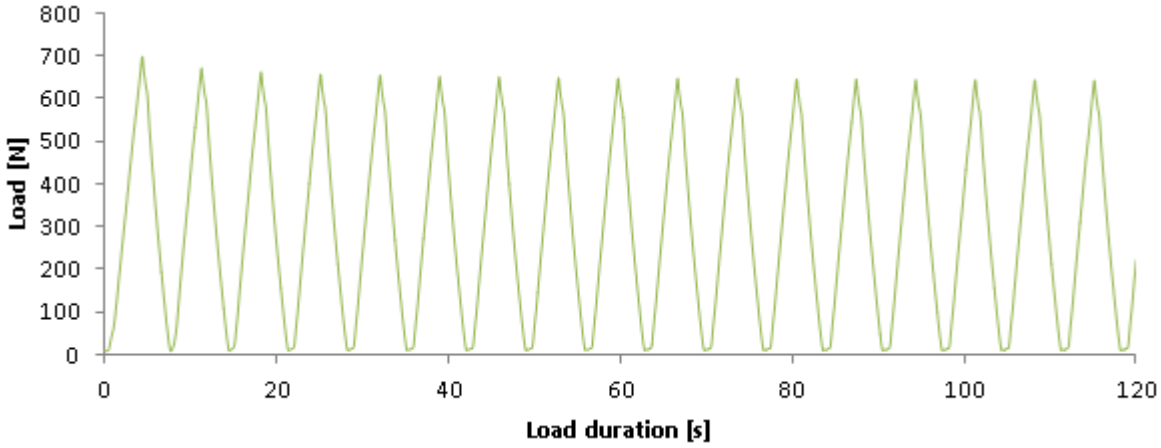

Figure 5.8 – Load response through time (0,144Hz)

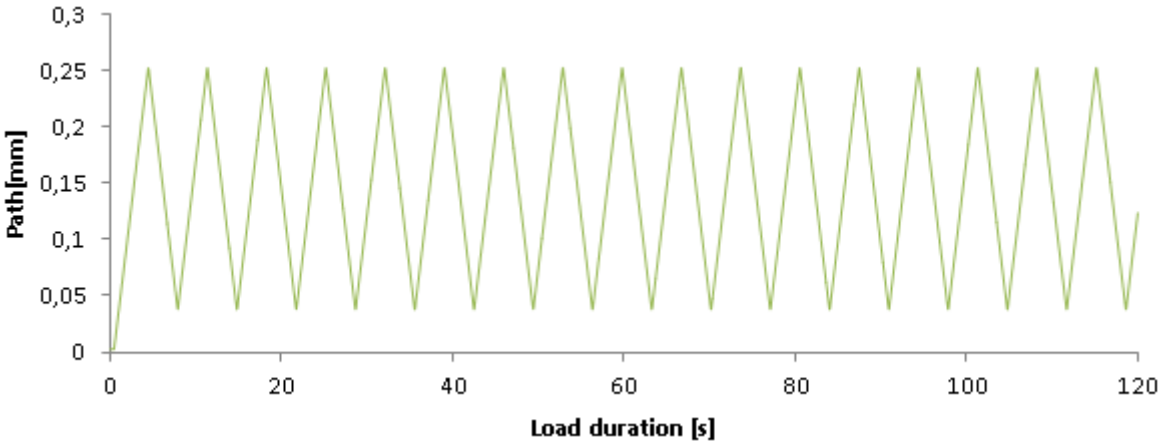

Figure 5.9 – Path condition through time (0,144Hz)

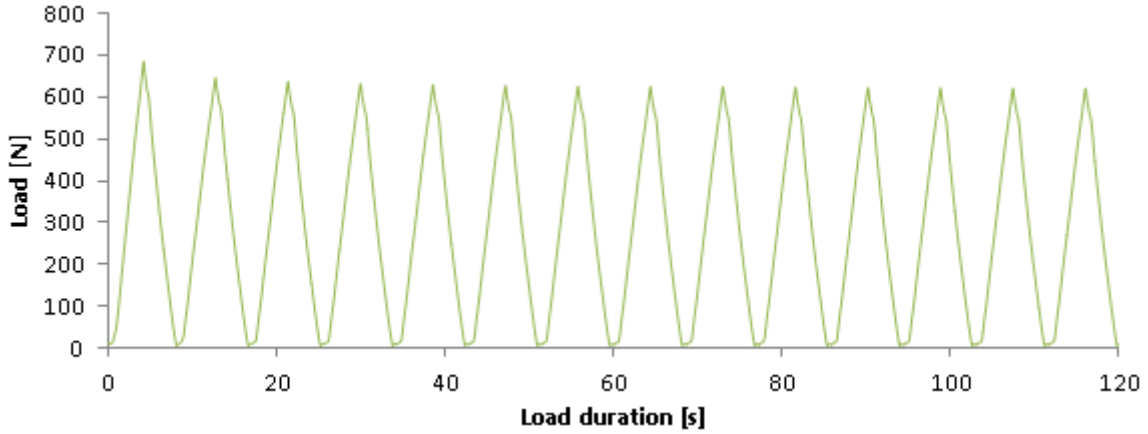

Figure 5.10 – Load response through time (0,117Hz)

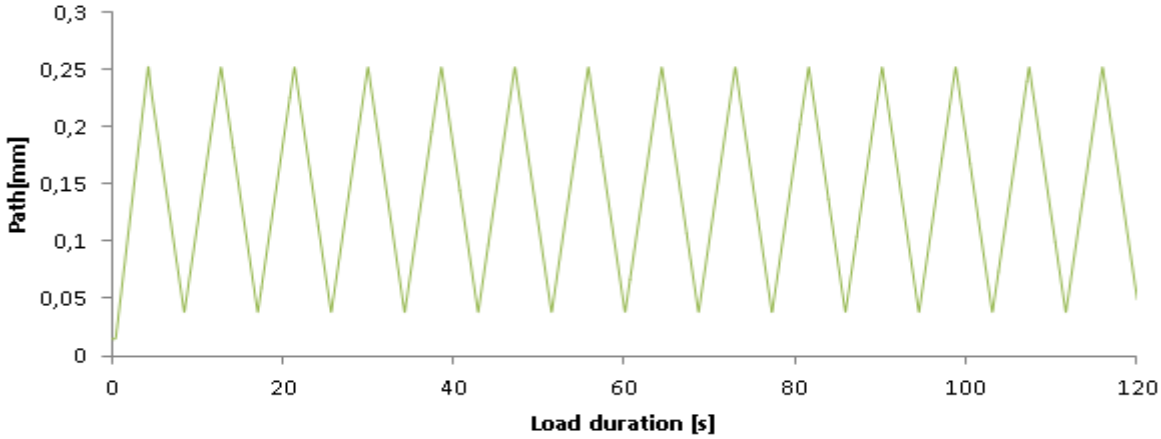

Figure 5.11 – Path condition through time (0,117Hz)

Table 5.1 – Frequencies tested

Freq. [Hz]	0,535	0,283	0,192	0,144	0,117

The following Figure 5.12 exhibits the trend for the constant behavior of PVB according to the range of tested frequencies. It is easy to conclude that the PVB interlayer, also as any other material in civil engineering, exhibits different response in accordance to different load frequencies. The amplitude at which the load response tends to stabilize decreases with the frequency.

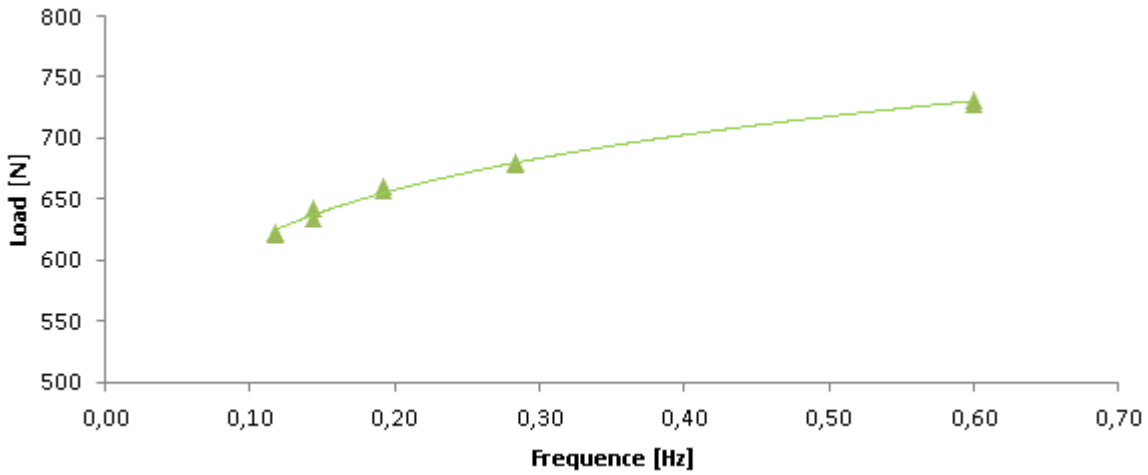

Figure 5.12 – Constant load response of the specimen through a range of frequencies

5.2 Large-Strain Tests

Large-strain force controlled tests were performed on laminates and float glass. The objective of those tests is to experimentally determine the specimen's fatigue time in presence of different load forces and then by means of *power law* make a numerical prognosis. In order to determine the failure stress for the laminates to be used in the analytical prognosis a FEM elastic model for static and cyclic loading was performed.

5.2.1 Dynamic Fatigue

Other float glass specimen were also tested in a dynamic way (Table A.1) in parallel with the laminates (for every two laminates tested till failure a float glass specimen was tested) in order to verify the sharpness of the indentation tool also as to verify de FEM numerical model for float glass. The middle value of the stress at which the specimens failed was of 43,22MPa, which is quite near the intended value (45MPa) and therefore verifies the sharpness of the diamond. The following Figure 5.13 compares the failure stress obtained from the experimental data of the with the regression line from the FEM numerical model presented in sub-chapter 4.4.1. It is evident that the experimental data of follows almost strictly the numerical regression line, that is, verifying the FEM numerical model and confirming that the float glass specimens after the indentation is applied have practically a linear load vs. stress relation.

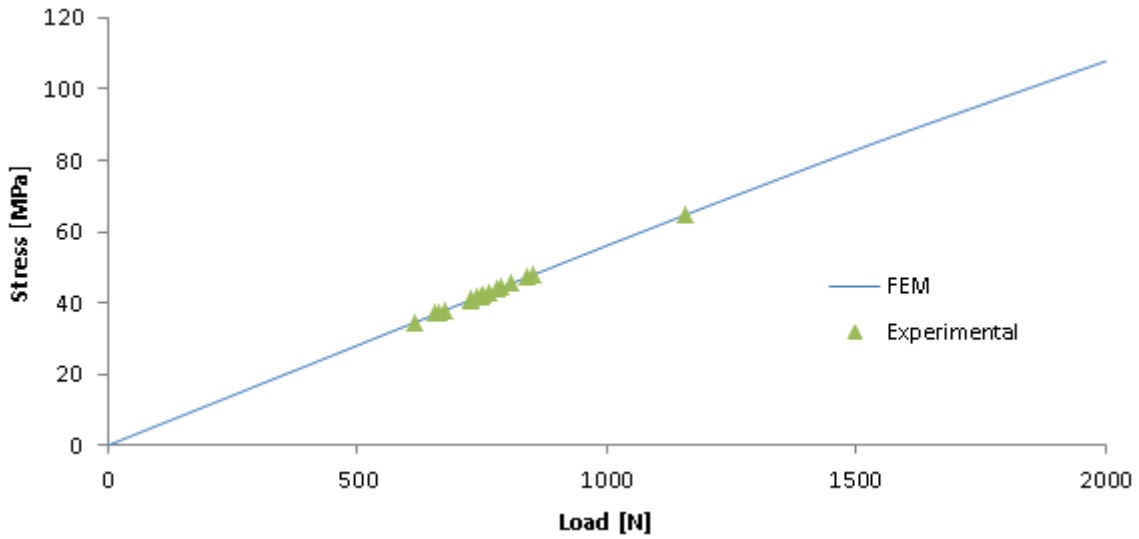

Figure 5.13 – FEM model vs experimental data

Those dynamic tests have also another function which is to determine the initial crack's depth induced by the flaw. For that the other *power law* parameters were assumed to be A=0,01 and Y=1,99 [5.]. With N previously determined to be 11,28, the failure load in terms of stress ($\sigma_{f,d}$) and the failure time (t_f) extracted from the experimental data, results the initial crack depth a_0 as presented in the Table A.1. Those constant values and the middle value of the initial indentation depth, a_0 = 1,63E-05m, were further utilized for the large strain fatigue predictions of the laminate specimen.

5.2.2 Static Fatigue

The Table A.2 presents the experimental data for the static fatigue. For forces below 800N, the specimen didn't fail for the imposed time limit of 100000s.

In order to define the static failure stress to be used in the *power law* (Table A.3) a FEM elastic model was performed for two conditions, which correspond to instances that were extracted from the experimental data. The first one corresponds to the instant at which the load force is achieved (t = 4s) and the second one corresponds to the instant before the failure of the specimen ($t = t_f$ or t = 100000s). With this approach it would be expected that the experimental data lies in between the two prediction limits resulting from the mentioned time instances (Figure 5.14).

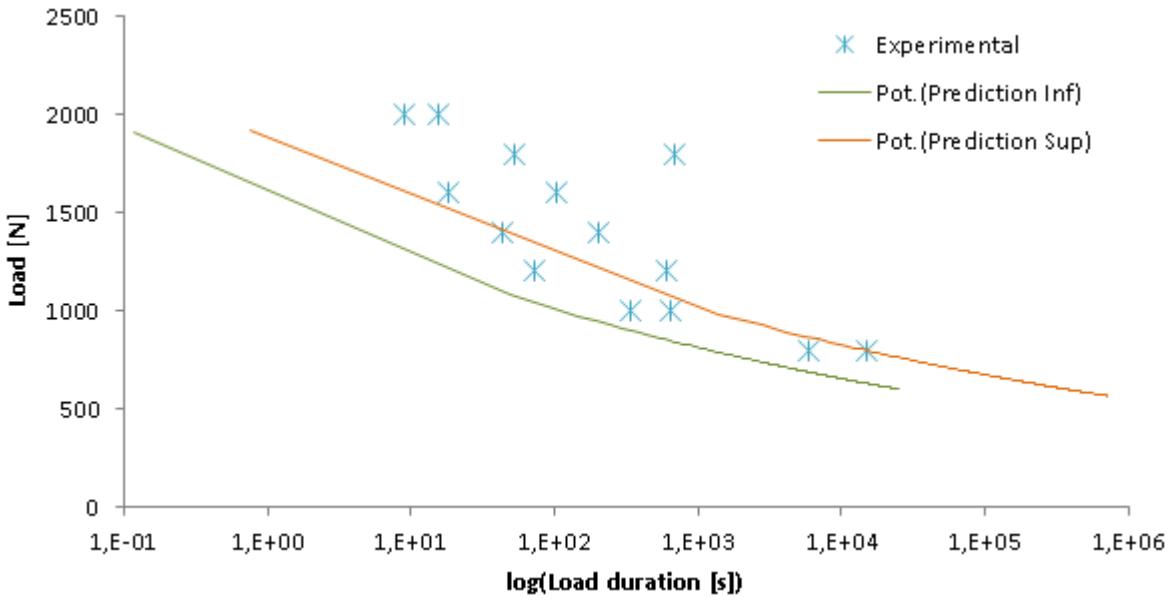

Figure 5.14 – Static fatigue: prognosis vs. experimental data

Most of the experimental results follow the tendency of the analytical *power law*, showing a better adjustment for the lower load forces.

5.2.3 Cyclic Fatigue

In order to perform cyclic force controlled tests for large-strain, the results from the static path controlled tests for small-strain where analyzed, that is, the long term stress (12,9MPa) and its respective load (528N) where considered. As the indentations were applied in order for the specimens to fail for the short term fatigue stress which means that the maximum load that should be considered in the cyclic force controlled tests, should be around four times the long term load from the static path controlled tests for small-strain (2500N). The experimental data is exposed in the Table A.4.

In order to define the cyclic failure stress to be used in the *power law* the FEM elastic model was performed for the maximum path amplitude (0,25) and the before mentioned constant load response extracted from the experimental data. After applying the ζ factor, which was determined to be 0,8, the static failure stress is obtained and the estimated failure time can be calculated Table A.5. The following Figure 5.15 exposes the experimental data and the resulting numerical prediction.

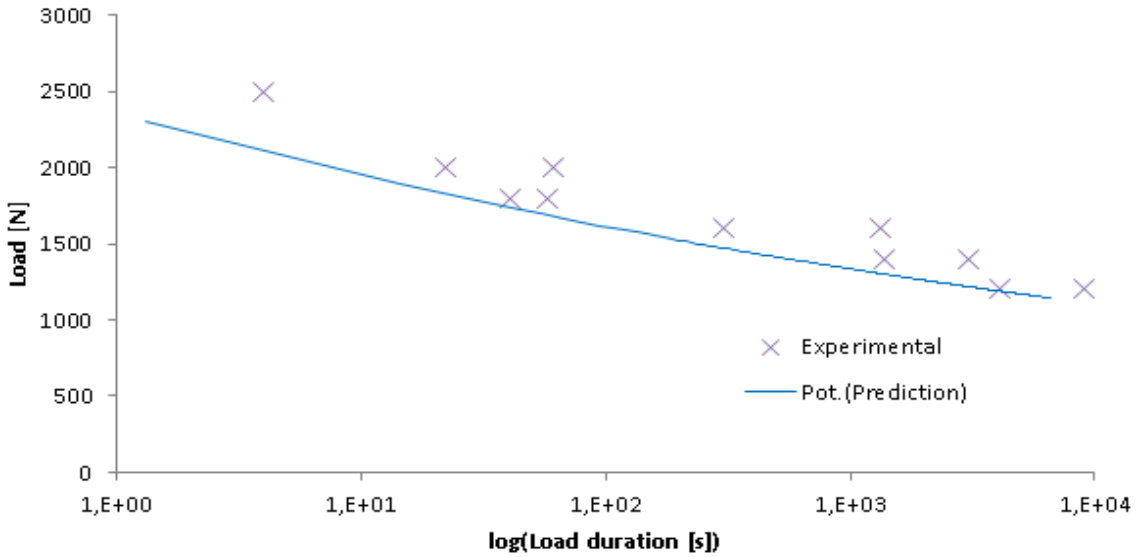

Figure 5.15 – Cyclic fatigue: prognosis vs. experimental data

The experimental results follow the tendency of the analytical *power law*, showing a good adjustment, although a little bit lagged, throughout the range of load forces.

6 SUMMARY AND OUTLOOK

The theme of this thesis was experimental and numerical investigation of the static and cyclic fatigue of laminated glass. The goal was to experimentally investigate the laminates fatigue and then to verify the FEM models. In order to achieve this objective experimental investigation for dynamic fatigue on float glass was also performed. The approach for the experiments was for the static test to be force controlled and the cyclic to be path controlled as it was easier to create the FEM models. For the prediction a combination of the FEM elastic model and the *power law* were of essence. In order to obtain statistically more concentrated results the specimens were pre-damaged via two indentations. Specimens that failed due to another flaw would be recognized and excluded.

The mesh study of the FEM models was performed for static force controlled conditions with the objective of obtaining the response for the deformation and the stress. It was concluded that the sizing of the mesh doesn't have a feasible impact on the results.

From the experimental data and FEM model for the float glass specimens it was concluded that the induced flaw needs to be applied with a indentation force of 435mN in order for the

specimens to break in the presence of the short term failure stress. Further the crack velocity parameter *N* was calculated to be 11,28.

For small-strain static path controlled tests it was concluded that the stress values obtained from the FEM viscoelastic and elastic were higher than the ones obtained through experimental data. The FEM elastic model results were closer to the experimental data and that is why for large-strain tests only the elastic model was considered. In order to obtain more coherent values between the FEM models and the experimental data the material properties of the PVB interlayer need to be investigated.

For small strain cyclic path controlled tests it was observed that the maximum response shows a brief initial decrease following by a constant maximum response. That is because the PVB experiences a long enough resting period and so recovers its material properties. The cyclic behavior of the laminate is much different than the static one, it doesn't present the substantial long term response decrease. The maximum response amplitude is frequency dependent and diminishes with it.

For large-strain dynamic force controlled tests the sharpness of the diamond was verified and via the *power low* and a middle value of 1,63E-05m was extracted for the initial crack depth. This value was further implemented in fatigue prediction for the laminates.

For large-strain static force controlled tests, with the used approach, the prediction tends to give better results for lower forces than for higher ones.

For large-strain cyclic force controlled tests, the prediction looks to be lagged in comparison to the experimental data.

This thesis can be used as a basis or a starting point for further research related with static or cyclic fatigue on laminated glass. In order to make even better fatigue predictions it would be prudent to investigate extensively the interlayer's material properties. It would be of interest to perform cyclic fatigue tests with other frequencies or load functions for float laminates, also as for tempered glass laminates.

REFERENCES

[1.] M. Haldimann, A. Luible, M. Overend (2008): Structural Use of Glass, Structural Engineering Documents; Zürich, Switzerland

[2.] M. Ciccotti (2009): Stress-corrosion mechanisms in silicate glasses; Université Montpellier 2, Montpellier, France
[3.] J. Varner (1996): Fatigue and Fracture Behavior of Glass, Fatigue and Fracture of Composites, Ceramics and Glasses, p 955-960; New York State College of Ceramics at Alfred University, New York, United States of America
[4.] X. Shen, (1997): Entwicklung eines Bemessungs- und Sicherheitskonzepts für den Glasbau, Fortschritt-Berichte; Darmstadt, Germany
[5.] F. Viehl (2012): Untersuchung des Ermüdungsverhaltens von gezielt vorgeschädigtem Floatglas; Technische Universitätt Darmstadt, Darmstadt, Germany
[6.] Y. Staudt (2013): Untersuchung des Materialverhaltens von Klebeverbindungen mit Silikon; Technische Universitätt Darmstadt, Darmstadt, Germany
[7.] B. Tsrankov (2012): Trageverhalten von Leichtglas mit SGP-Ywischenshiecht; Technische Universitätt Darmstadt, Darmstadt, Germany
[8.] C. Vallabhan, Y. Das, M. Ramasudra (1992): Properties of PVB Interlayer Used in Laminated Glass, J. Mater. Civ. Eng., p 71-76; Texas Tech University, Texas, United States of America
[9.] J. Barredo, M. Soriano, M. Gómez, L Hermanns (2011): Viscoelastic Vibration Damping Identification Methods. Application to Laminated Glass; Politechnic University of Madrid, Madrid, Spain
[10.] A. Duser, A. Jagota, S. Bennison (1999): Analysis of Glass/Polyvinyl Butyral Laminates Subjected to Uniform Pressure; J. Eng. Mech., p 435-442; E.E. DoPont de Nemours & Co., Inc., Wilmington, DE, Wilmington, United States of America
[11.] P. Hooper, B. Blackman, J. Dear (2012): The Chemical Behavior of Poly(Vinyl Butyral) at DifferentStrain Magnitudes and Strain Rates; J. Mater. Sci., p 3564-3576; Imperial College London, London, United Kingdom
[12.] P. Sternberg (2013): Untersuchung de Delaminationsverhaltens vo Polyvinylbutyral; Technische Universitätt Darmstadt, Darmstadt, Germany
[13.] A. Engel (2011): Untersuchung der Festigkeit von Planmäßig Vorgeschädigtem Glas; Technische Universitätt Darmstadt, Darmstadt, Germany
[14.] http://en.wikipedia.org/wiki/Laminated_glass (28.06.2014)
[15.] http://en.wikipedia.org/wiki/Polyvinyl_butyral (28.06.2014)
[16.] Trosifol® (2012): Technical Manual: The Processing of Trosifol® PVB Film; Kuraray Europe Gmbh Division Trosifol®, Troisdorf, Germany
[17.] http://www.ewp.rpi.edu/hartford/~ernesto/F2012/MEF2/Z-Links/Pics/Fracture/FractureModes.png (28.06.2014)
[18.] K. Pankhardt (2010): Load Bearing Glasses; Budapest University of Technolody and Economics, Budapest, Hungary

[19.] V. Sackmann, C. Schuler, H. Gräf (2005): Testing of laminated safety glass, Fachhochschule München, München, Germany
[20.] J. Hilcken, J. Schneider (2014): Untersuchung von Kalk-Natron-Silikatglas bei schwingender Beanspruchung, Glas in Konstruktiven Ingenieurbau 12; Technische Universitätt Darmstadt, München, Germany
[21.] G. Molnár, L. G. Vigh, G. Stocker, L. Dunai (2012): Finite Element Analysis of Laminated Structural Glass Plates With Polyvinyl Butyral (PVB) Interlayer, Per. Pol. Civil Eng., p 35-42; Budapest University of Technology and Economics, Budapest, Hungary
[22.] K. Hoffmann (): Hinweise zur Inatallation von Dehnunsmessstreifen (DMS); Germany
[23.] Brinsen (polymers)
[24.] J. Hilcken (2014): Zyklische Ermüdung von thermisch entspanntem und thermisch vorgespanntem kals-Natro-Silikatglas, Werkstoffmechanik-Seminar; Technische Universitätt Darmstadt, Trifels, Germany
[25.] R. Kennedy (1997): The history and future of the flat glass industry, Proceeding of Glass Processing , p 13-15; Tampere, Finland
[26.] http://www.neatorama.com/2012/09/10/The-History-of-Glass/#!bqDo70 (30.07.2014)
[27.] http://krex.k-state.edu/dspace/bitstream/handle/2097/471/RachelWhite2007.pdf%20rel=%27nofollow%27?sequence=1 (30.07.2014)
[28.] http://www.sglavo.it/Contacts/Vetro/STV0607/flat%20glass.PDF (30.07.2014)
[29.] B. Weller, F. Nicklisch and J. Wünsch (2009): Dynamic behaviour of adhesives for structural glass applications; Glass Performance Days, p 366-370, Technical University of Dresden, Dresden, Germany

Annex

Table A.1 – Dynamic fatigue results and definition of the initial crack depth

Load [N]	t_f [s]	$\sigma_{f,d}$ [Mpa]	a_0 [m]
841,60	23,67	47,33	2,67E-05
675,15	18,99	37,97	4,79E-05
657,44	18,49	36,98	5,14E-05
1156,10	32,51	65,02	1,15E-05
852,43	23,97	47,94	2,58E-05
746,92	21,00	42,01	3,67E-05
809,52	22,76	45,53	2,96E-05
750,87	21,12	42,23	3,62E-05
764,00	21,48	42,97	3,45E-05
787,86	22,16	44,31	3,18E-05
725,94	20,41	40,83	3,95E-05
616,82	17,35	34,69	6,08E-05
778,45	21,89	43,78	3,29E-05
729,59	20,52	41,03	3,9E-05
663,20	18,65	37,30	5,02E-05
739,05	20,78	41,57	3,77E-05

Table A.2 – Static fatigue results for laminated glass

Load [N]	t_f[s]
2000	8,9
2000	15,6
1800	51,8
1800	690,7
1600	18,2
1600	102,0
1400	202,9
1400	43,0
1200	606,6
1200	71,5
1000	635,9

1000	342,1
800	15037,2
800	5970,0
700	>100000
600	>100000

Table A.3 – Static fatigue prognosis for laminated glass

Load [N]	$\sigma_{f,s,inf}$ [MPa]	$\sigma_{f,s,sup}$[MPa]	t_f[s]	t_f[s]
2000	42,2	53,05	1,55	0,12
2000	44,9	52,73	0,77	0,13
1800	41,95	51,17	1,66	0,18
1800	43,2	51,20	1,19	0,18
1600	36,5	43,27	7,98	1,17
1600	36,67	45,70	7,57	0,63
1400	33,23	40,65	23,00	2,37
1400	33,87	40,50	18,55	2,47
1200	27,1	35,00	229,47	12,81
1000	23,8	29,50	992,74	88,11
1000	26,45	29,60	301,76	84,81
800	23,43	23,12	1184,65	1376,70
800	17,33	22,33	35561,06	2037,78
700	15,73	20,86	106052,88	4392,96
600	13,31	17,90	698062,02	24685,41

Table A.4 – Cyclic fatigue results for laminated glass

Load [N]	t_f [s]
2500	4,0
2000	22,0
2000	60,7
1800	58,0
1800	41,0
1600	1325,0
1600	302,0
1400	3027,0
1400	1378,0
1200	9000,0
1200	4060,0

Table A.5 – Cyclic fatigue prediction for laminated glass

Load [N]	$\sigma_{f,d}$ [MPa]	$\zeta\sigma_{f,d}$ [MPa]	t_f[s]
2500	53.5	42.83	1.31
2000	45.35	36.31	8.47
2000	47.7	38.19	4.79
1800	40.32	32.28	31.88
1800	41.15	32.95	25.34
1600	36.05	28.86	112.70
1600	38.93	31.17	47.36
1400	31.16	24.95	583.50
1400	34.15	27.34	207.57
1200	25.8	20.66	4906.26
1200	25.12	20.11	6631.31